AD-A079 792 ARMY ELECTRONICS RESEARCH AND DEVELOPMENT COMMAND WS--ETC F/G 4/1
SHORT-TIME MASS VARIATION IN NATURAL ATMOSPHERIC DUST.(U)
NOV 79 T L BARBER
UNCLASSIFIED ERADCOM/ASL-TR-0045 NL

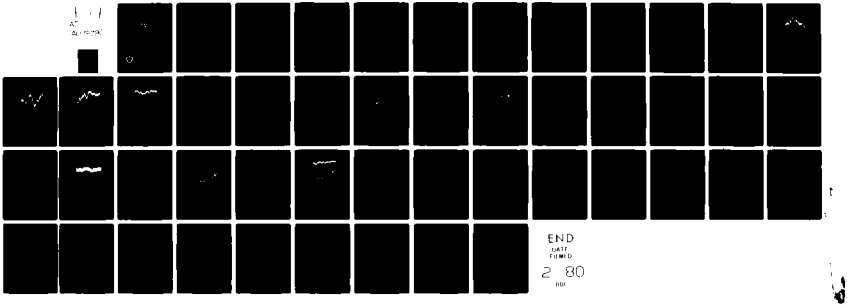

END
DATE FILMED
2 80
DDC

ASL-TR-0045

AD

Reports Control Symbol
OSD 1366

AD A079792

LEVEL I

SHORT-TIME MASS VARIATION IN NATURAL ATMOSPHERIC DUST

NOVEMBER 1979

By
TEDDY L. BARBER

Approved for public release; distribution unlimited

US Army Electronics Research and Development Command
ATMOSPHERIC SCIENCES LABORATORY
White Sands Missile Range, NM 88002

NOTICES

Disclaimers

The findings in this report are not to be construed as an official Department of the Army position, unless so designated by other authorized documents.

The citation of trade names and names of manufacturers in this report is not to be construed as official Government indorsement or approval of commercial products or services referenced herein.

Disposition

Destory this report when it is no longer needed. Do not return it to the originator.

SECURITY CLASSIFICATION OF THIS PAGE *(When Data Entered)*

REPORT DOCUMENTATION PAGE

READ INSTRUCTIONS BEFORE COMPLETING FORM

1. REPORT NUMBER: ASL-TR-0045
2. GOVT ACCESSION NO.
3. RECIPIENT'S CATALOG NUMBER
4. TITLE *(and Subtitle)*: SHORT-TIME MASS VARIATION IN NATURAL ATMOSPHERIC DUST
5. TYPE OF REPORT & PERIOD COVERED: Technical Report
6. PERFORMING ORG. REPORT NUMBER
7. AUTHOR(s): Teddy L. Barber
8. CONTRACT OR GRANT NUMBER(s)
9. PERFORMING ORGANIZATION NAME AND ADDRESS: Atmospheric Sciences Laboratory, White Sands Missile Range, NM 88002
10. PROGRAM ELEMENT, PROJECT, TASK AREA & WORK UNIT NUMBERS: DA Task 1L161102B53A
11. CONTROLLING OFFICE NAME AND ADDRESS: US Army Electronics Research and Development Command, Adelphi, MD 20783
12. REPORT DATE: November 1979
13. NUMBER OF PAGES: 38
14. MONITORING AGENCY NAME & ADDRESS *(if different from Controlling Office)*
15. SECURITY CLASS. *(of this report)*: UNCLASSIFIED
15a. DECLASSIFICATION/DOWNGRADING SCHEDULE

16. DISTRIBUTION STATEMENT *(of this Report)*

Approved for public release; distribution unlimited.

17. DISTRIBUTION STATEMENT *(of the abstract entered in Block 20, if different from Report)*

ERADCOM/ASL-TR-0045

18. SUPPLEMENTARY NOTES

19. KEY WORDS *(Continue on reverse side if necessary and identify by block number)*

Lidar
Atmospheric dust
Dust variation
Particulate backscatter
Aerosol structure

20. ABSTRACT *(Continue on reverse side if necessary and identify by block number)*

Aerosols are not perfectly mixed in the atmosphere, but reside in miniclouds, even in a relatively clear atmosphere.

This report presents a mathematical treatment relating mass loading to optical backscatter, and some of the inherent problems in examining light scattering from natural dust in a theoretical manner are discussed.

DD FORM 1 JAN 73 1473 EDITION OF 1 NOV 65 IS OBSOLETE

410 663

1 SECURITY CLASSIFICATION OF THIS PAGE *(When Data Entered)*

20. ABSTRACT (cont)

CONT

Lidar backscatter data were taken in a desert environment and related to mass loading variations over 30-second periods. Four of the 30-second segments of the data are presented. In these four segments, the estimated relative mass loading was observed to fluctuate up and down with the highest mass loading about eight times that of the lowest mass loading. These mass loading fluctuations were observed at one position 15 meters above the ground.

ACKNOWLEDGMENTS

The author thanks Dr. H. Auvermann, Physical Science Laboratory, New Mexico State University, for his advice and assistance in computer programming.

The author also thanks Dr. R. Pinnick, Atmospheric Sciences Laboratory, White Sands Missile Range, New Mexico, for his advice and guidance on light-scattering matters.

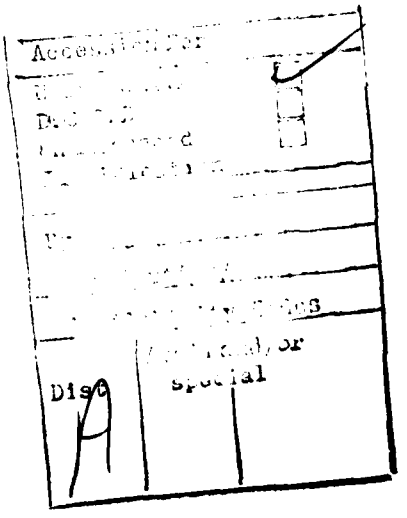

CONTENTS

INTRODUCTION

The primary purpose of the experiment on short-time mass variation in natural atmospheric dust was to remotely measure winds in the atmosphere; however, this report covers a facet of the effort relating measured backscatter to relative mass loading changes in the atmosphere. This relationship was made by observing the motion of dust irregularities through two well-defined scattering volumes of a lidar. The lidar is a laser radar device which projects a light beam into the atmosphere and, with an optical receiver, collects and monitors the backscattered light. In a short time period, the change in backscatter can be related to the change in the mass loading of dust, under the assumption that the form of particle size distribution is time-invariant. The dust in the atmosphere affects a number of atmospheric processes. The heat balance of the atmosphere is noticeably affected by the dust. Dust can be active in gas-particle reactions or as a catalyst. Certain types of natural dust can react with man-made pollutants; for example, calcite will readily react with sulfuric acid fumes. Dust particles can act as condensation nuclei in the growth of haze, fog, or cloud particles. A knowledge of the mass distribution of the natural dust is useful in other studies of chemical and physical processes in the atmosphere. By taking the backscatter information from one beam of the lidar, the author examined the short-term (1 to 10 seconds) mass variation of natural dust in the atmosphere. The relative mass fluctuations and horizontal physical sizes of the dust irregularities were estimated. These dust variations were measured on the evening of 4 December 1977 at White Sands Missile Range (WSMR), New Mexico, at a position 15 meters above the ground.

A mathematical development relating backscatter and mass concentration in a relatively clean atmosphere is presented. The backscatter from a known volume of the atmosphere was measured relative to time. The wind was measured simultaneously near the backscatter volume for the purpose of inferring horizontal dimensions and wind shear at the edge of the irregularities.

BACKGROUND

Researchers have been interested in the dust in the atmosphere for many years. When the Krakatoa volcano in the South Pacific erupted in 1883, ejecting tons of dust into the high atmosphere, people from many parts of the earth could observe the effects of the scattered light after dusk. By noting the first time this colorful effect could be seen in each of several places, researchers estimated dust motion. This occurrence was one of the early qualitative observations of dust motion in the atmosphere.[1] More recently, investigators have probed the atmosphere both horizontally and vertically with an airborne laser radar to examine large-scale horizontal layering.[2] Using a laser radar system, Collis was able

---

[1] "Krakatoa," Encyclopedia Britannica, 1959, 13:498-499

[2] F. G. Fernald and B. G. Shuster, 1977, "Wintertime 1973 Airborne Lidar Measurements of Stratospheric Aerosols," J Geophys Res, 82:3

to observe airflow and diffusion rates of artificially produced aerosol clouds in a mountain valley.[3] This permitted a more thorough knowledge of micrometeorological conditions in the valley. Derr and Little,[4] using a bistatic two-beam lidar system, examined the backscatter from clear atmosphere and found a substantial degree of correlation between two specific scattering volumes. Within the past 3 years, scanning laser radars[5] have been used to examine the horizontal and vertical motion of large-scale backscatter variations in the atmosphere. Lidar measurements have been made to a height of more than 1000 meters, and horizontal ranges of up to 10 kilometers.

In many years of taking lidar data, Murray* has observed that relatively sharp irregularities in the backscattered return occur almost all of the time. From this observation, it can be inferred that dust irregularities in the atmosphere are quite common.

THEORY

Four of the pioneers in the basic theory development of light scattering from particles in a medium were Clebsch, 1863;[6] Rayleigh, 1871;[7]

---

[3]Ronald T. H. Collis, 1968, "Lidar Observations of Atmospheric Motion in Forest Valleys," Bull Am Meteorol Soc, 49:918

[4]V. E. Derr and C. G. Little, 1970, "A Comparison of Remote Sensing of the Clear Atmosphere by Optical, Radio and Acoustic Radar Techniques," Appl Opt, 9(9):1976-1985

[5]T. G. Leuthner and E. W. Eloranta, 1977, "Remote Measurements of Longitudinal and Crosspath Wind Velocities with a Monostatic Lidar," paper presented at the Eighth International Laser Radar Conference at Drexel University, Philadelphia, PA, June 1977

*E. R. Murray, personal communications, March 1979, Stanford Research Institute, Menlo Park, CA

[6]A. Clebsch, 1863, J Fur Math, 61:195

[7]Lord Rayleigh, 1912, The Scientific Papers of Lord Rayleigh, 1 and 4, Cambridge University Press, NY

Mie, 1908;[8] and Debye, 1909.[9] A rather thorough history of the early workers in light scattering has been compiled by Kerker.[10] Today, the theory of single scattering from a spherical homogeneous particle carries the name Mie theory.

The natural dust is a mixture of minerals, a few of which are calcite, dolomite, kaolinite, montmorollinite, quartz, gypsum, and thenardite.[11] However, at the present stage of development of the lidar method, one must assume that the dust consists of homogeneous spheres all with the same refractive index.

Three specific approximations are made to meaningfully interpret lidar results. These approximations concern the refractive index, m, the particle size distribution, and particle shapes.

The refractive index, $m = n - ik$, where n is the real portion ordinarily measured on refractometers, is important in backscattering computations. (All terms used are explained in the definition of symbols at the end of the report.) Values of n in the visible light region are specific to given minerals[12] and vary according to wavelength. An extended discussion of the relation between the average m and extinction of light is given by Toon et al[13] who examine the error on extinction related to the average m when minor components of the dust deviate markedly from this average. A reasonable average value for n for dust of the type observed at

---

[8]G. Mie, 1908, "Beitrag zur optik trüber medien, speziell kolloidaler metallosungen," Ann Phys, 25:377-445

[9]P. Debye, 1909, "Das verhalten von lichtwellen in der nähe eines brennpunktes oder einer brennlinie," Ann Phys, 30:755-776

[10]M. Kerker, 1969, The Scattering of Light and Other Electro-Magnetic Radiation, Academic Press, NY

[11]G. B. Hoidale, S. M. Smith, A. J. Blanco, and T. L. Barber, 1967, "A Study of Atmospheric Dust," ECOM Report 5067, Atmospheric Sciences Laboratory, White Sands Missile Range, NM

[12]Esper S. Larsen and Harry Berman, 1934, "The Microscopic Determination of the Nonopaque Minerals," Bulletin 848, US Department of the Interior, Geological Survey

[13]Owen B. Toon, James B. Pollack, and Carl Sagan, 1977, "Physical Properties of the Particles Composing the Martian Dust Storm of 1971-1972," Icarus, 30:663-698

WSMR is 1.52.[14] The value of k in the visible light spectral region is small compared to n and is related directly to the Beer's law absorption of the material, providing particles are small compared to the wavelength.[15] The average value of k in the visible region which has been measured for specific dust types at WSMR is approximately 0.01.[16] A knowledge of m is important since particulate backscatter is a sensitive function of this parameter.

The second problem is that which arises with changes in size distribution that occur in the natural atmosphere with various changes in meteorological conditions. Since the data presented in this research work cover only a few minutes of time, these changes in size distribution are probably not a major problem. For interpreting the lidar results, the size distribution is assumed to be constant during this period.

The third area of approximation is in the particle shape. The Mie theory pertains to homogeneous spheres; the problem of irregularly shaped dust particles causes a difference relative to exact Mie theory. Chýlek et al[17] have examined the problem of irregular shape relative to perfect spheres. The difference between backscatter from irregular dust particles as compared to spheres of equal cross section can be as much as a factor of 2 to 5. This is simply a difference between scatter from irregular particles and spheres. Slightly irregular dust particles with equivalent size parameter $X(X = 2\pi r/\lambda)$ of 3 or less can be closely approximated by the Mie theory for scattering as found by Pinnick et al.[18]

The backscatter cross section B_{180} is a function of size parameter X, the size distribution f(r), the index of refraction m, and the total number of particles in the scattering volume N_o. As previously mentioned, the size distribution of dust can change radically with a change in meteorological conditions. Over a few hours of time, for example 24 hours, this assumption of the constancy of f(r), the size distribution, would be

---

[14]G. W. Grams, I. H. Blifford, Jr., D. A. Gillette, and P. B. Russell, 1974, "Complex Index of Refraction of Airborne Soil Particles," J Appl Meteorol, 13:459-471

[15]S. G. Jennings, R. G. Pinnick, and J. B. Gillespie, 1979, "Relation Between Absorption Coefficients and Imaginary Index of Atmospheric Aerosol Constituents," Appl Opt, 18(9):1368-1371

[16]James D. Lindberg and James B. Gillespie, 1977, "Relationship Between Particle Size and Imaginary Refractive Index in Atmospheric Dust," Appl Opt, 16:2628-2630

[17]Peter Chýlek, G. W. Grams, and R. G. Pinnick, 1976, "Light Scattering by Irregular Randomly Oriented Particles," Science, 193:480-482

[18]R. G. Pinnick, D. E. Carroll, and D. J. Hofmann, 1976, "Polarized Light Scattered from Monodisperse Randomly Oriented Non-Spherical Aerosol Particles: Measurements," Appl Opt, 15(2):384-393

invalid. At the other extreme, this approximation is accepted during 1 second of time while a small volume of the atmosphere is being considered, for example 1 cubic meter. Gillette* has examined size distribution variations in natural dust in conditions of relatively high visibility in time periods as short as 10 seconds. He found essentially no variation in the size distribution over several tens of seconds. For the individual time periods of 30 seconds from figures 1 through 4, this approximation that f(r) is constant is assumed to be reasonable under reasonably stable meteorological conditions. The data presented in this report cover only a few minutes of time; and over this period, wind conditions, temperature, and atmospheric pressure conditions were essentially constant.

For the case being considered here, the differential size distribution f(r) is a function that will produce the fraction of particles with size r. The relation between backscattered radiation and the mass loading can be derived by assuming that the particle size distribution f(r) will not change appreciably during the total time period of . minutes for which data are presented.

For spherical particles,

$$B_{180} = \frac{N_o}{4\pi} \int_{r_1}^{r_2} G\pi r^2 \, f(r)dr, \qquad (1)$$

where B_{180} is the total backscatter cross section in the volume of interest, G is the ratio of the geometrical cross section of a particle to its effective backscatter cross section, and πr^2 is the cross section of a single particle.

For a specific size distribution of material, G is a specific function. The mass of dust is defined as

$$M = N_o P \int_{r_1}^{r_2} \frac{4}{3} \pi r^3 \, f(r)dr, \qquad (2)$$

*D. A. Gillette, April 1979, personal communications, unpublished data, National Center for Atmospheric Research, Boulder, CO

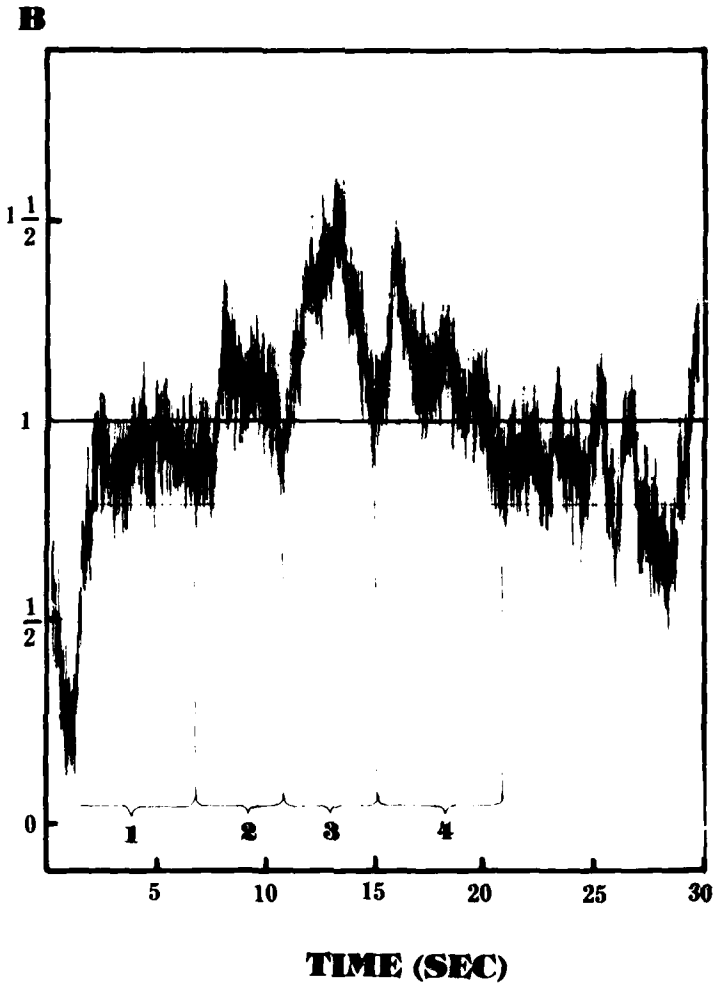

Figure 1. Backscatter data, from a volume in the atmosphere 2 cm in diameter and 4 m long.

The data presented in figure 1 were taken at the rate of 6000 samples per second on the evening of 4 December 1977. For this graph, 50 points were summed and divided by 50 as a new data point. Scale B is a relative scale based on the theory section. The average, or the 1 on scale B, is an average over 2 minutes of data. The size of these dust cells is obtained by comparing the anemometer chart with this graph, obtaining an average windspeed for a time period and therefore the size. The more definite dust cells maximum mass loading and size are listed in table 3. These cells are indicated by the numbers on this figure. Cross-correlation with this and the adjacent scattering volume obtained a correlation maximum of 0.85.

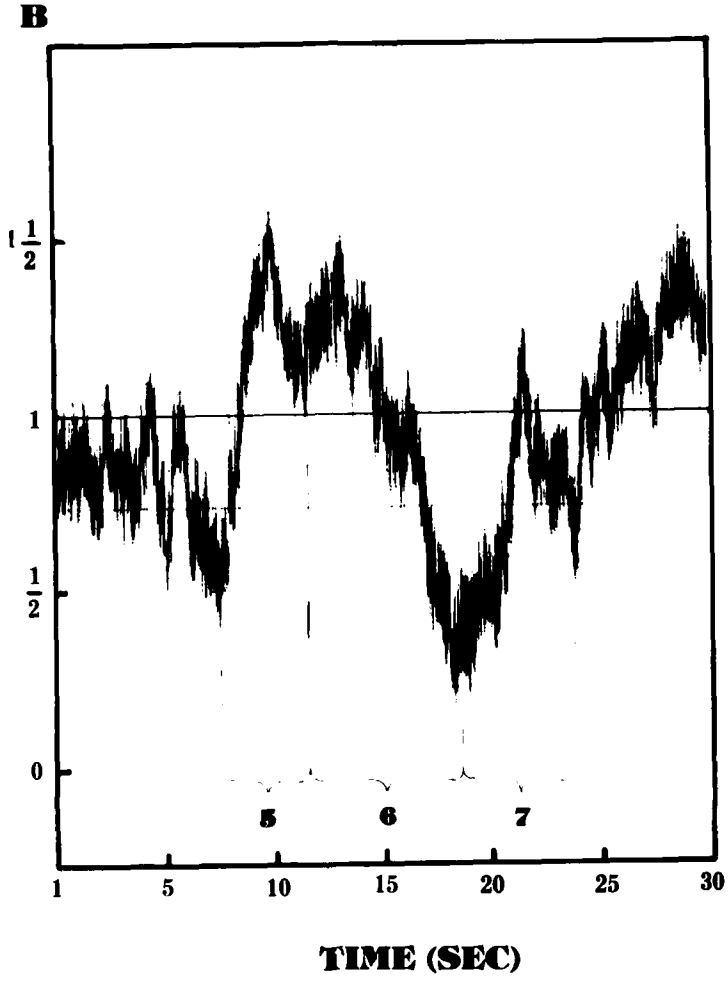

Figure 2. Time depiction of backscatter data from a volume in the atmosphere.

The graph continues from figure 1; parameters given in figure 1 still apply. Zero time in this figure is the 26th second in figure 1. Cross-correlation with this and the adjacent scattering volume obtained a correlation maximum of 0.87.

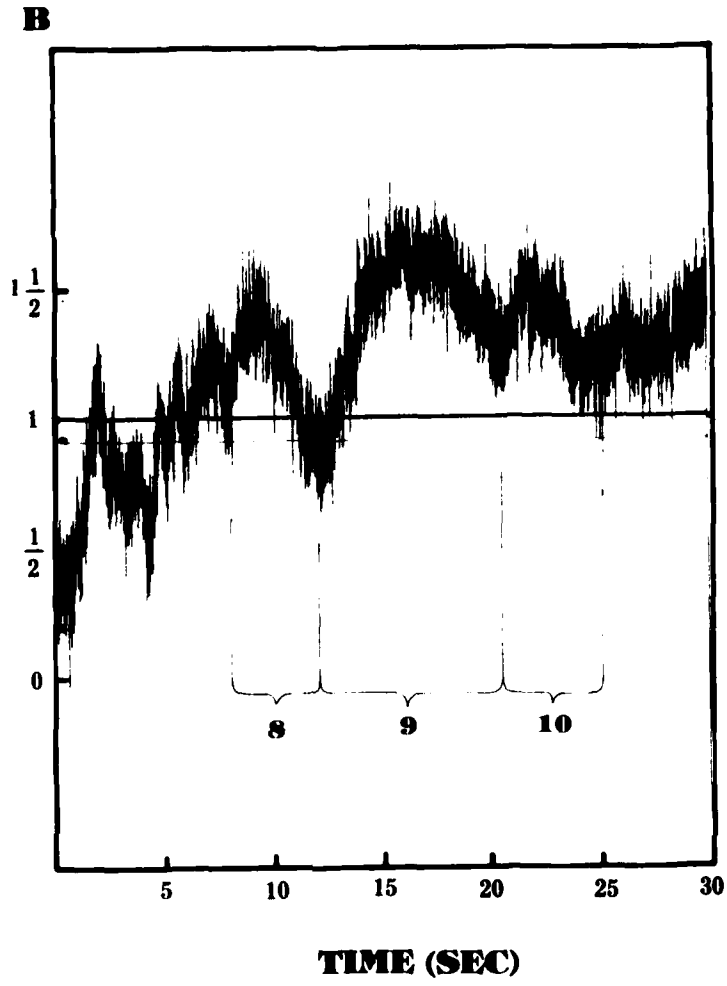

Figure 3. Time depiction of backscatter data from a volume in the atmosphere.

The graph continues from figure 2; parameters are the same as in figure 1. Zero time in this figure is the 18th second in figure 2. Cross-correlation with this and the adjacent scattering volume obtained a correlation maximum of 0.94.

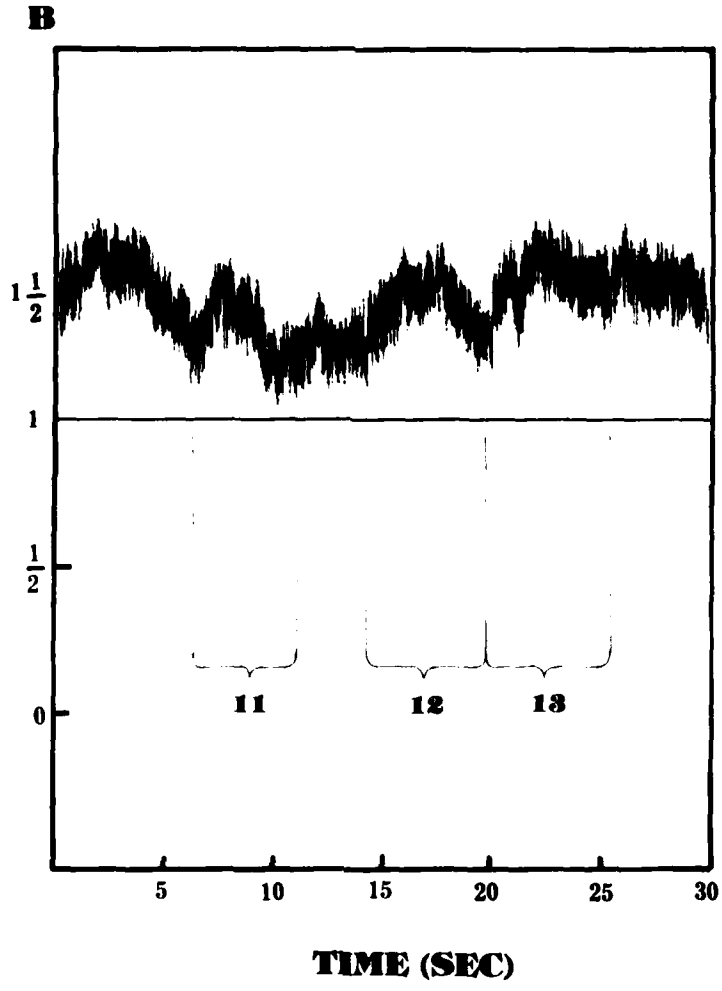

Figure 4. Time depiction of backscatter data from a volume in the atmosphere.

The graph continues from figure 3; parameters are the same as in figure 1. Zero time in this figure is the 15th second in figure 3. Cross-correlation with this and the adjacent scattering volume obtained a correlation maximum of 0.99.

where M is the total mass of dust in a specific volume (mass loading) of air, P is the average density of the dust, and the other terms are as defined above for equation (1).

With a specific $f(r)$,

$$B_{180} = D_3 M \ , \tag{3}$$

where D_3 is a proportionality factor, or

$$\frac{B_{180}}{M} = D_3 \ . \tag{4}$$

From equations (1) and (2),

$$\frac{B_{180}}{M} = \frac{\frac{N_o}{4} \int_{r_1}^{r_2} Gr^2 f(r) dr}{N_o P \frac{4}{3}\pi \int_{r_1}^{r_2} r^3 f(r)\, dr} \ . \tag{5}$$

Assuming the same r_2 to r_1 limits in both numerator and denominator, equation (5) can be simplified to

$$\frac{B_{180}}{M} = \frac{\frac{1}{4} D_1}{P \frac{4}{3}\pi D_2} = D_3 \ , \tag{6}$$

where D_1 and D_2 are separate numbers which depend on the form of the differential size distribution $f(r)$; hence, the whole function on the right side of equation (6) is a specific number.

The effect of dust scattering losses on the laser beam and return signal will now be considered. The quantity that is measured is not B_{180} directly. With a constant laser energy E, from the lidar,

$$B_{180}E = S \ , \tag{7}$$

where S is the signal available at the front of the receiver for a condition in which transmission losses are zero. The transmission losses in the atmosphere are now considered. There is some small amount of light extinction in the outgoing laser beam and in the return scattered beam.

The extinction coefficient, σ, can be obtained by the Koschmieder[19] relation, which relates visibility, V, to the extinction coefficient,

$$V = \frac{3.912}{\sigma} \ . \tag{8}$$

During the time the backscattering data were taken, the horizontal visibility V was estimated to be 130 kilometers. The total transmission T is related to the extinction coefficient by the relation

$$T = e^{-2\sigma L} \ . \tag{9}$$

T is the fraction of the total light that will traverse the distance of interest. L is the range from lidar to scattering volume or 0.07 kilometer. The number 2 is inserted because the laser beam goes out and the scattered light must return to the receiver.

Using equations (8) and (9) with L = 0.07 kilometer,

$$T \approx 0.996 \ . \tag{10}$$

This transmission is the atmospheric transmission, and it is essentially 1, so that the extinction can be neglected in the expression for the lidar return signal.

EXPERIMENTAL

The objective of this segment of the investigation was to measure and record the backscatter from a fixed volume in the atmosphere. The

[19]H. Koschmieder, 1924, "Theorie der horizontalen Sichweite," Beitr Phys freien Atm, 12:33-53, 171-181

general device was a lidar. The transmitter source was a copper vapor laser, transmitting at 5106 and 5782 angstroms. About three-quarters of the total power was produced at 5106 angstroms. The total power averaged around 5 watts. This laser was a pulsed device, with a 20-nanosecond-long pulse, operated at 6000 pulses per second.

Figures 5 and 6 are general diagrams of the experimental setup. This relatively isolated spot on the White Sands Missile Range was chosen to get away from man-made sources of dust to work with more natural conditions.

The collimator and detector assembly are shown in figure 7. With the collimator, a beam diameter of 2 centimeters was obtained at 70 meters range, putting all of the available energy through the scattering volumes. The director mirror permitted careful pointing of the laser beam so as to illuminate the sample volume that the telescope saw efficiently. The size of the sample volume in the atmosphere was 2 centimeters diameter and 4 meters long.

The backscattered signal from the volume of interest was collected by a 75-centimeter-diameter Cassegrainian receiver telescope. The scattered light collected by the telescope was converted to an electronic signal by a photomultiplier. An electronic gate accepted only 27 nanoseconds of the signal from a range of 70 meters. Light travels 8 meters in 27 nanoseconds, 4 meters forward and 4 meters backward, thus defining the 4-meter length of the sample volume.

Figure 8 is a time depiction of the operation of the gate circuit. For a more thorough discussion of the receiver, photomultiplier system, and the gate circuit, the reader is referred to Barber and Mason.[20]

ANALYSIS AND RESULTS

With the backscattered signal received and recorded from the lidar, an estimated relative mass loading scale for dust in the atmosphere can be obtained. In the theory section, it was shown that the backscattered signal is proportional to the mass loading if the assumption is true that $f(r)$ is constant over a short period of time in a relatively small atmospheric volume. Because of the assumptions made, the exact value for the proportionality constant D_3 is not known; however, a linear relative scale can be developed.

Two specific factors are needed to relate the value of B_{180} to the actual backscattered signal that is received and recorded from the lidar. These are the laser output E and the efficiency of the receiver system, Z. As will be shown below, both are essentially constant for the conditions of the experiment.

---

[20]T. L. Barber and J. B. Mason, 1974, "A Transit-Time Lidar Wind Measurement: A Feasibility Study," ECOM Report 5550, Atmospheric Sciences Laboratory, White Sands Missile Range, NM

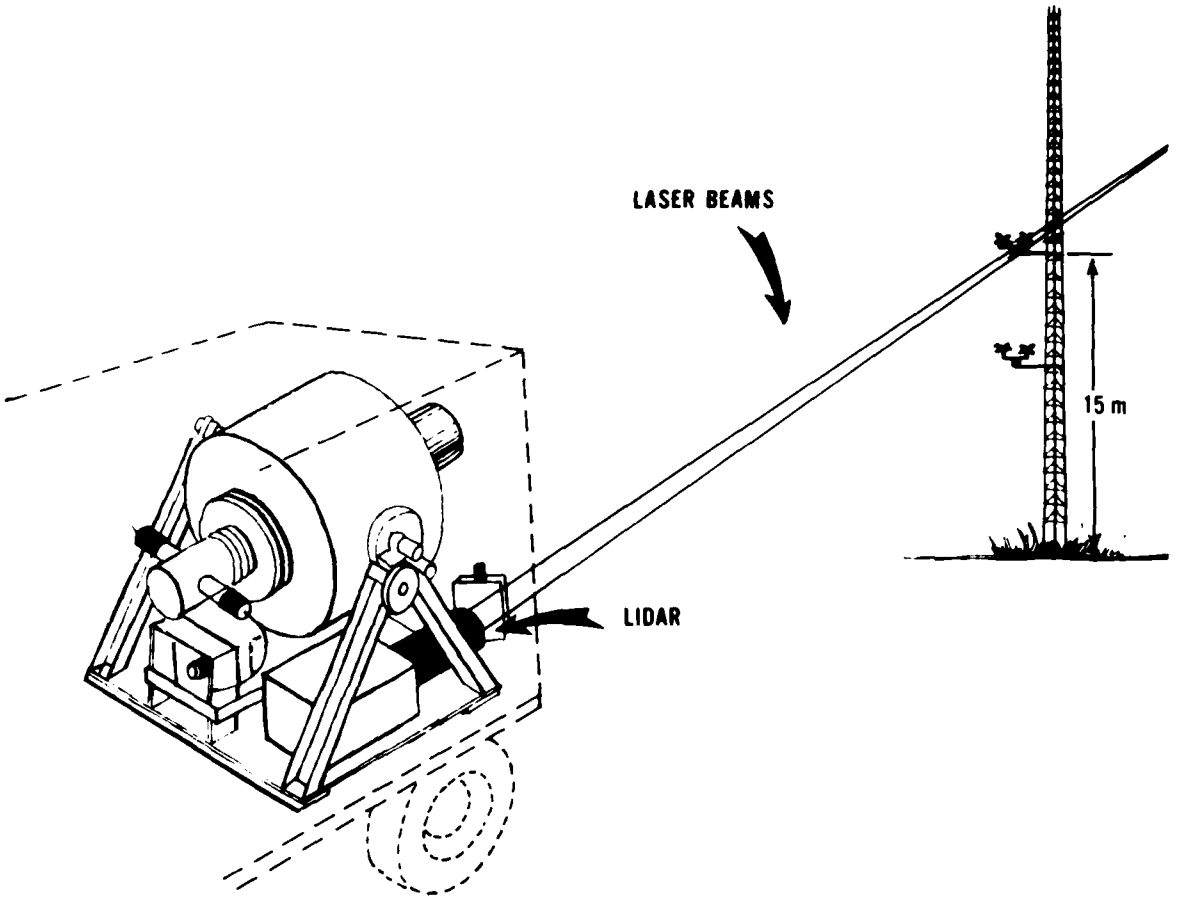

Figure 5. Experimental setup. The lidar consisted of a pulsed copper vapor laser transmitter and a 75-cm-diameter Cassegrainian receiver telescope. Two laser beams were projected outward and the scattering volume of interest was set to be horizontally adjacent to the reference anemometer. The backscattered signal picked up by the receiver telescope was converted to an electronic signal by a photomultiplier shown on the rear of the telescope.

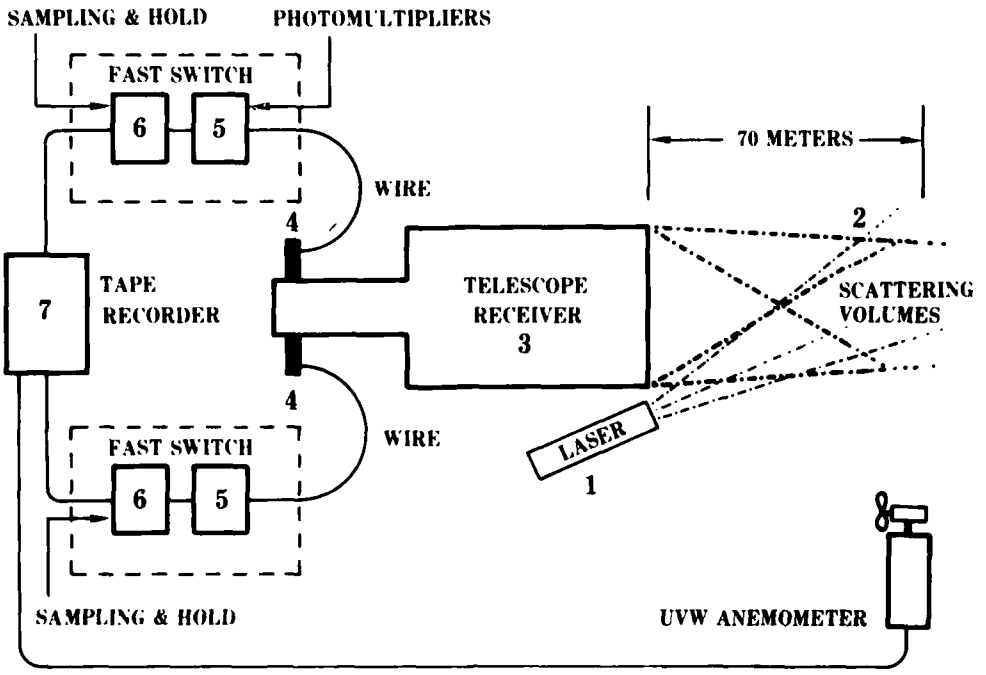

Figure 6. A layout of the lidar measuring system.

1. The copper vapor laser transmitter
2. The two scattering volumes in the free atmosphere, 15 meters above the ground.
3. The receiver telescope
4. The photomultiplier
5. The fast gate switch which defines the range L
6. The sample and hold network holding the average signal for 100 micro-seconds.
7. The tape recorder

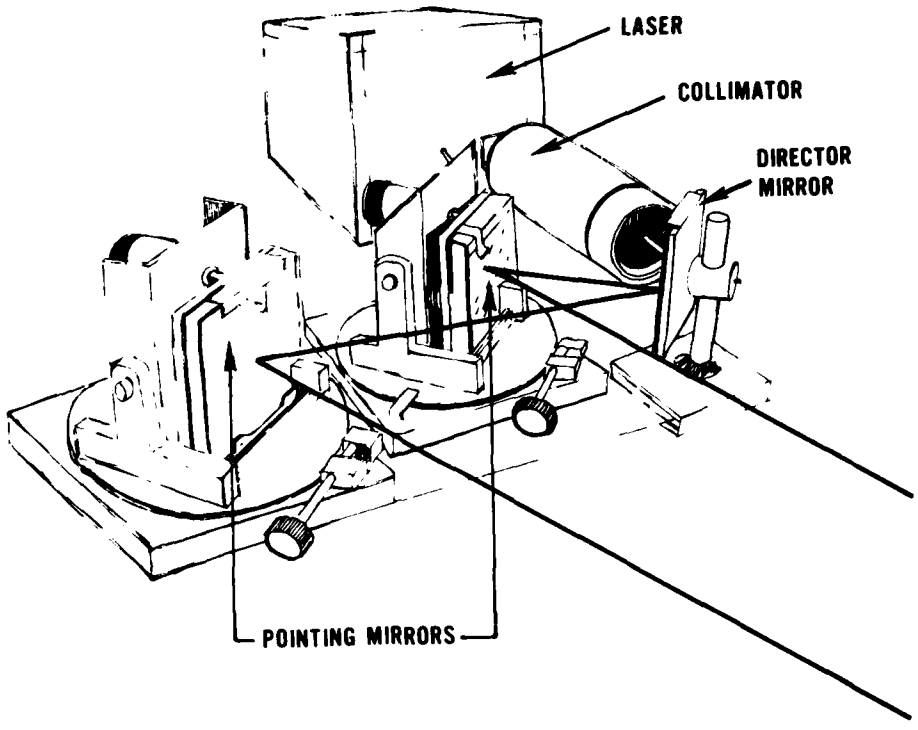

Figure 7. Copper vapor laser, collimator, and pointing mirrors. For this experiment only, information from mainly one of the two beams was used. The collimator permitted a more efficient use of the laser energy. The pointing mirror allowed an adequate illumination of the sample volume.

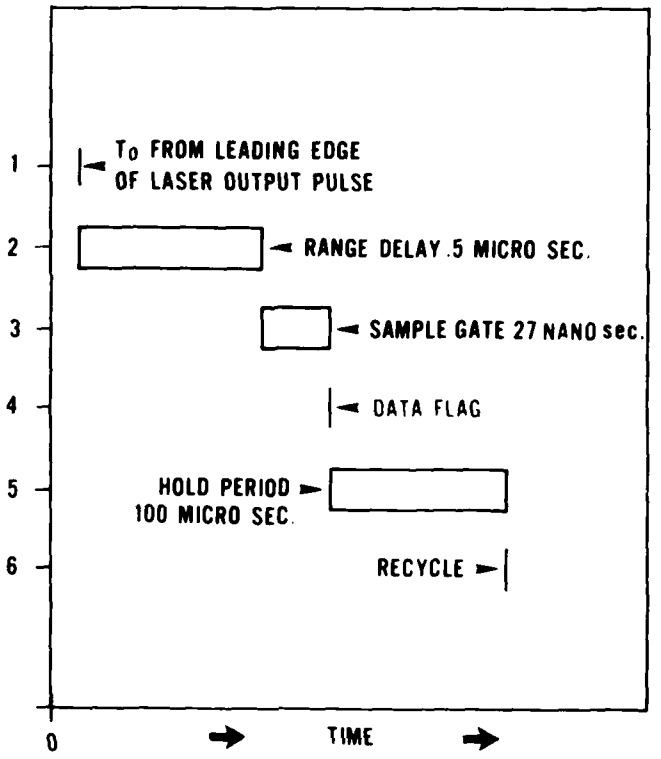

Figure 8. A time depiction of the gate circuit operation.

The backscatter signal, electronic, produced by the photomultiplier, was processed by this circuit. Step 1 was an electronic pulse produced by a light-sensitive diode in the laser. Step 2 was the time delay from laser pulse production to the area at the scattering volume, 0.5 microsecond. Step 3, a fast switch turned on passing 27 nanoseconds of the signal from the photomultiplier. Step 4 was a reference pulse to trigger the A - D converter. In step 5, the signal was held for recording by an analog recorder for later processing.

It was determined that the short-time variation of the laser output E was less than 5 percent. Therefore, E can be considered constant over the 2- to 3-minute time period of the experiment.

The efficiency Z includes the mirror surface efficiencies of the primary and secondary telescope mirrors, the transmission efficiencies of the optical filter, the gain of the photomultiplier tube, and the efficiency of the gate circuit system, values for which are given in the definition of symbols. The linearity and reproducibility of the photomultiplier tube, its biasing network, and the gate were measured by putting three different intensity values of pulsed light into the tube and monitoring the gate voltage. There was less than 1 percent variation from linearity and of reproducibility. With this measurement, Z can be considered a constant.

Taking E as a constant,

$$B_{180}E = S \ , \tag{7}$$

where S is the signal that reaches the receiver telescope. The actual recorded voltage will be equal to the signal S divided by the efficiency factor Z; that is, $S = ZV_1$. It then follows from equation (7) that

$$B_{180}E = ZV_1 \ . \tag{11}$$

Using equations (3) and (11),

$$M\left(\frac{D_3E}{Z}\right) = V_1 \ . \tag{12}$$

The portion in parentheses is constant only if the size distribution f(r) is constant. V_1 is the recorded voltage from the gate circuit.

In figures 1 through 4, there is a relative scale B, based on equation (12), linear and proportional to the backscattered return. The data average for both average M and average B_{180} for this total time period of 2 minutes is placed at the value 1 on the scale. An average mass loading value based on a mass measurement over the same 2-minute time period must be known to relate mass loading units to the relative dust backscatter scale B. There are several available methods to estimate an average mass loading value in the atmosphere, but these are for much longer time periods.

Table 1 shows the contribution of particles of various sizes to the backscatter and mass loading (Knollenberg counter data[21]). The Knollenberg counter is an electronic device which utilizes light scatter to measure and count particles. The effect of different values of k (the imaginary index of refraction) on the backscatter cross section is also illustrated in this table. A value can be obtained from the data giving an average mass loading of 34.5 micrograms per cubic meter over a 10-minute time period, but this value is statistically weak.

Hinds and Gillespie* have measured mass loading values by drawing a known volume of air through a millipore filter over a 2-week period and weighing the resultant material on the filter. Their values taken about 5 kilometers west of the lidar site during the period July 1975 to July 1976 are presented in table 2.

An average mass loading value can also be estimated, knowing a value for the horizontal visibility[22] at the time the lidar data were taken; during this time the horizontal visibility was approximately 130 kilometers.

The following equation (from reference 22) relates the horizontal visibility V to the mass loading M and gives an estimate of the average mass loading:

$$M = \frac{1.8 \times 10^3}{V} . \qquad (13)$$

From this equation, there are estimated deviations of $\pm$50 percent.

The value from table 2, the first set of data for rather clear air in the fall, would be about 21 micrograms per cubic meter. In method 3, the value obtained by using the horizontal visibility was 14 micrograms per cubic meter. From table 1, a mass loading can be obtained from this counter data, taken only 3 days after the backscattering data in similar meteorological conditions. This value is 34.5 micrograms per cubic meter. The wide disagreement in these values indicates that further work must be done to determine the cause of the discrepancies. It then may be possible to accurately relate B_{180} to M. Since this is not now possible, it is necessary to deal with relative mass loadings rather than absolute ones.

---

[21]R. G. Pinnick and H. J. Auvermann, 1979, "Response Characteristics of Knollenberg Light-Scattering Aerosol Counters," J Aerosol Sci, 10:55-74

*B. D. Hinds and J. B. Gillespie, Feb 1979, personal communication, unpublished data, Atmospheric Sciences Laboratory, US Army Electronics Research and Development Command, White Sands Missile Range, NM

[22]Robert J. Charlson, N. C. Ahlquist, H. Selvidge, and P. B. Macready, Jr., 1969, "Monitoring of Atmospheric Aerosol Parameters with the Integrating Nephelometer," J Air Poll Control Assoc, 19:937-942

TABLE 1. KNOLLENBERG DUST COUNTER DATA

Channel Number	Channel Count	X	Channel Center (μm)	Channel Width (μm)	Mass per Channel ($\mu g\ m^{-3}$)	$B_{180} \cdot 10^{-8}\ m^{-1}SR^{-1}$ n = 1.5		
						K = 0	K = 0.05	K = 0.1
1	214	1.93	0.157	0.04	0.65	6.9	9.0	2.8
2	96	2.43	0.198	0.04	0.54	32.7	18.0	14.4
3	24	2.95	0.24	0.04	0.24	10.8	3.8	1.0
4	17	3.52	0.286	0.055	0.31	30.1	7.6	2.5
5	16	3.57	0.29	0.08	1.65	7.6	1.2	0.24
6	12	5.03	0.41	0.17	0.34	45.0	9.2	2.8
7	4	9.85	0.8	0.6	0.97	93.0	5.1	1.0
8	3	19.7	1.6	1.0	5.53	--	--	--
9	1	44.0	3.6	3.1	24.34	--	--	--

The dust particle counter data from table 1 were taken at the same position as the scattering volumes, with the exception of 2 meters displacement horizontally. The data were taken 7 December 1977 at 9:00 p.m. Five 2-minute segments of data were averaged to produce this set. Data for channels 1 through 4 were from measurements made with a Knollenberg Model No. ASASP-300. Data for channels 5 to 9 were produced from measurements made by a Knollenberg Model CSAP-100. The count number is the number of particles the counter saw in that radius range. $X = 2\pi r/\lambda$, the size parameter. Channel center represents the average particle radius. Channel width is the dimension from the smallest to the largest particle counted in that channel. Mass per channel is the mass loading for all the particles in that size range.

$$M_b = \frac{C\,P}{\pi r F T_s} \int_{r_1}^{r_2} \frac{4}{3}\pi r^3\, dr\ ,$$

$$B_{180} = \frac{C}{\pi r F T_s} \frac{1}{4\pi} \int_{r_1}^{r_2} G \pi r^2\, dr\ ,$$

P is the average density of the dust particles.

C is the number of particles counted in that size range.

B_{180} is the total backscatter cross section of all the particles in that size range.

G is the backscatter gain averaged over that channel.

r_2 is the larger limit in the channel.

r_1 is the small limit in the channel.

T_s is the sampling time, and F is the flow rate.

The three columns on the right represent different values of G obtained from a standard light scattering table[23] for specific values of n and k. This table lists values only to X = 15. Therefore, there are no values for the last two entries in these columns.

Statistically, this counting period T_s is too short in this clear air condition. In channel 9, it would be better to extend T_w where C becomes approximately 100.

[23] N. C. Wickramasinghe, 1973, Light Scattering Functions for Small Particles with Applications in Astronomy, John Wiley and Sons, NY

TABLE 2. AVERAGE MASS LOADING MEASUREMENTS

Date Taken	Mass Loading ($\mu g\ m^{-3}$)
1-15 July 1975	12
15-29 July 1975	11
29 July - 1 August 1975	11
11-25 August 1975	8
25 August - 8 September 1975	8
9-22 September 1975	8
22 September - 7 October 1975	19
7-22 October 1975	19
22 October - 3 November 1975	18
3-17 November 1975	24
17 November - 1 December 1975	27
1-15 December 1975	25
15-29 December 1975	--
29 December 1975 - 14 January 1976	14
14-26 January 1976	15
26 January - 9 February 1976	14
11-23 February 1976	16
23 February - 8 March 1976	51
9-22 March 1976	53
22 March - 6 April 1976	41
6-19 April 1976	45
19 April - 3 May 1976	30
3-17 May 1976	28
17 May - 1 June 1976	17
1-14 June 1976	24
14-28 June 1976	34

Mr. B. D. Hinds and J. Gillespie obtained and furnished these data from a site about 5 kilometers west of the lidar site. The sampler was on a tower 3.5 meters above the ground. Air was drawn through 47-millimeter plastic filters at a known rate, and the mass of the dust was obtained by weighing the filter. With this information, mass loading can be obtained. It must be remembered that this is an average over a 2-week period.

The 0 in the relative dust backscatter scale (figures 1 through 4) has been corrected for Rayleigh scatter, from gas molecules, and residual gate voltage. The Rayleigh scatter, from the literature,[24] is estimated to be 10 percent or less of the average backscatter. The value taken was 10 percent. The effect of this correction tends to compress the relative dust backscatter scale, which makes the relative backscatter changes occur over a larger relative mass range.

In a fast gate circuit as used here, there is a small but constant voltage on the gate, even when the input leads are shorted. This constant value is about 8 percent of the average signal during this time. The 0 was adjusted to eliminate both the estimated Rayleigh scattering signal and the gate residual voltage. The average value relates to the number 1 on the relative scale B. These corrections appear quite reasonable for the data obtained, since the lowest relative mass loading observed was still slightly above 0 after these corrections were applied (see figure 1).

Three comparisons were made to check the reliability of the data. As shown in figure 7, the laser beam was split into two beams. Each of these beams irradiated separate volumes in the atmosphere 24 centimeters apart at an identical range from the transmitter. A separate photomultiplier tube measured the light from each of these volumes. A separate group of electronics processed the signals, and the signals were recorded on separate channels in the tape recorder. During the computer processing, the two signals (figures 2 and 9) were cross-correlated (figure 10). At a maximum of the cross-correlation, a value of 0.85 or more was obtained; the cross-correlation maximum did not fall at zero time delay. This is important because if the cross-correlation maximum fell at zero time delay, it would indicate that these variations were caused by variations in the laser output. Rather, the time delay is an indication of the time of flight of the dust minicloud from one scattering volume to the other. The reason for the lag time was that the dust irregularities were being carried along by the wind; the wind took a certain period of time to carry these dust clouds through a distance of 24 centimeters, which was the beam separation.

Also, in the wind records taken simultaneously with this backscatter data, a change in the wind velocity can generally be seen to correlate with the edges of these dust clouds (figure 11). Weinman* proposed that there should be wind shear at the surface of these dust miniclouds.

---

[24]R. A. McClatchey, R. W. Fenn, J. E. A. Selby, F. E. Volz, and J. S. Garing, 1971, "Optical Properties of the Atmosphere (Revised)," AD 726116, AFCRL-71-0279, Environmental Research Papers, Air Force Cambridge Research Laboratories, L. C. Hanscom Field, Bedford, MA

*J. Weinman, personal communications, March 1978, Department of Meteorology, University of Wisconsin, Madison, WI

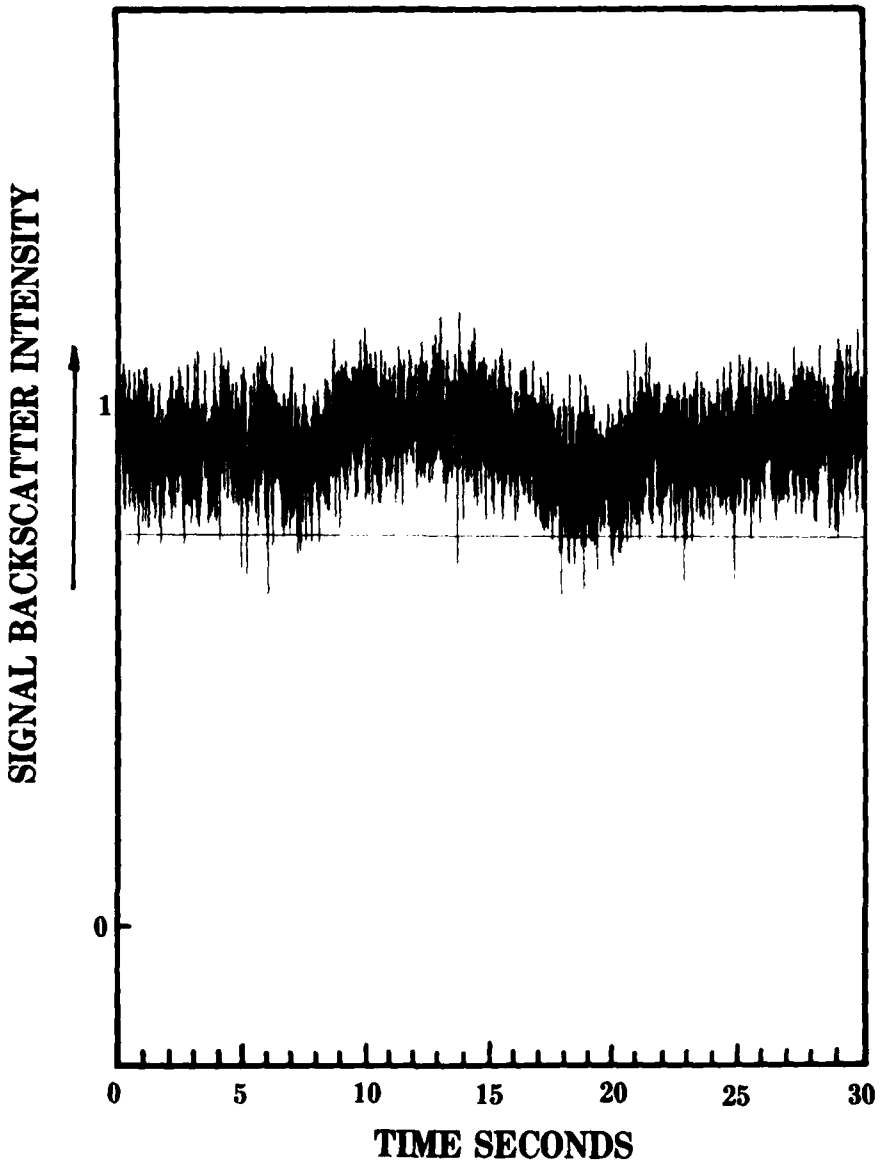

Figure 9. The raw backscattering data from the second scattering volume.

The raw signal from the first scattering volume is shown in figure 2. These data were taken simultaneously with the data in figure 2 and were cross-correlated with the data in figure 2 to obtain the correlation curve in figure 10. The difference between the two curves arises in the high frequency components in the data. The frequency components 5 hertz and higher are felt to be unrelated to the backscatter from the dust. Part of this discrepancy arises in that this channel, laser beam, and receiver were not quite as well aligned as the other channel. Also, during processing, the computer scaled these data about 25 percent smaller in amplitude.

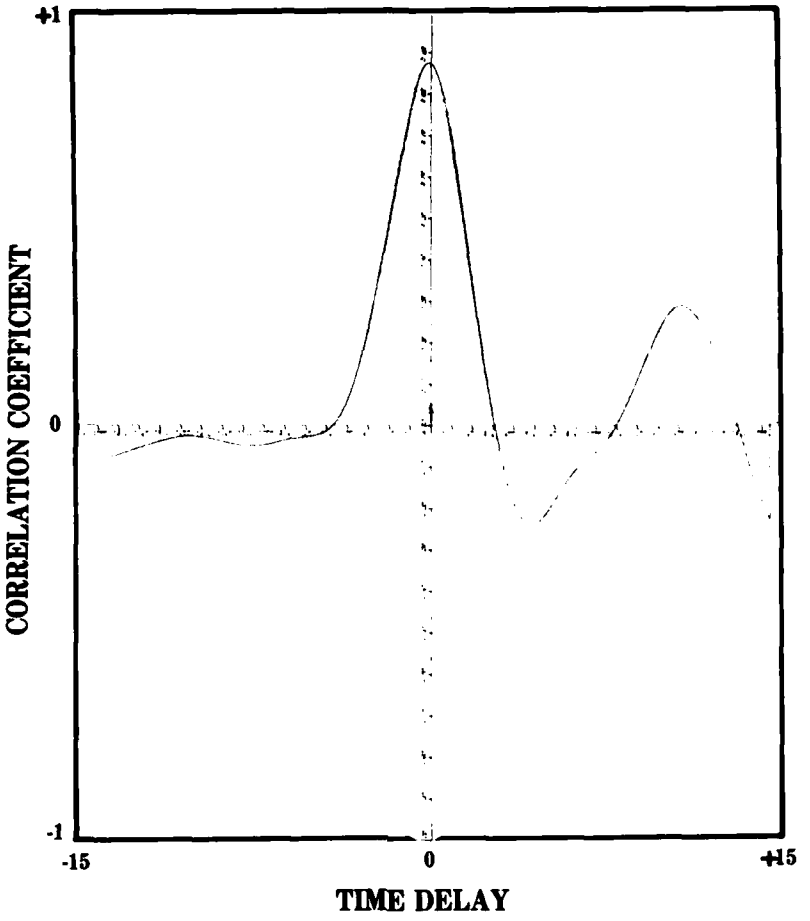

Figure 10. A cross-correlation of the data in figure 9 with the data in figure 2.

Results were obtained by placing a high frequency filter in the data with a $\cos^2$ roll-off. The 0.707 point in this filter was set at 1 hertz. The remaining signal was cross-correlated. The correlation maximum was 0.87 at a time lag of 0.1 second.

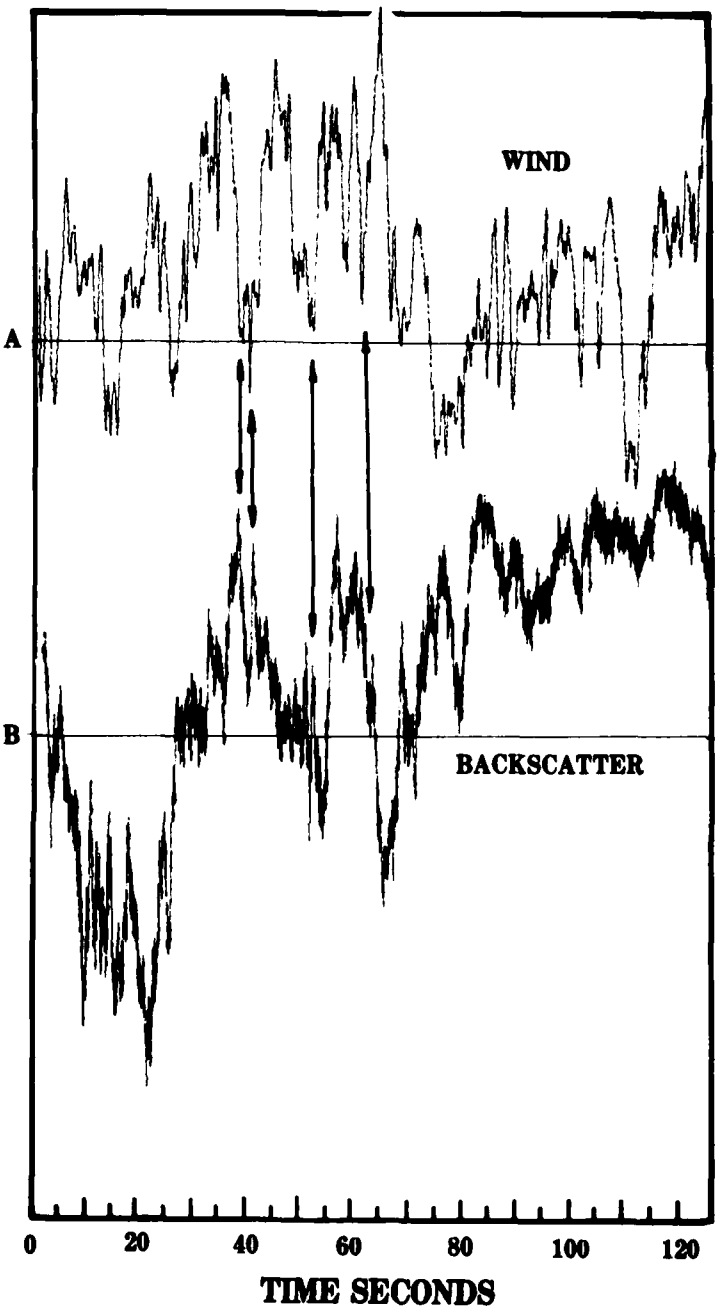

Figure 11. Three of the dust clouds that appear in the mass loading data are pointed out in the wind record (numbers 3, 5, and 6).

This wind record was taken simultaneously with the backscatter data having the instrument offset horizontally 2 meters from the scattering volume. Curve A is the wind record covering from 6 to 14 meters per second and the horizontal component of the wind perpendicular to the laser beam. Curve B is the backscatter data over the same period of time. This figure illustrates the wind shear at the edge of the dust miniclouds.

TABLE 3. MAXIMUM MASS LOADING OF DUST CLOUDS AND THEIR HORIZONTAL DIMENSIONS

Sample Number	Horizontal Dimension (m)	Mass Loading ($\mu g\ m^{-3}$)
1	58	24
2	38	28
3	44	37
4	24	32
5	56	35
6	42	33
7	50	27
8	40	34
9	31	40
10	72	37
12	38	37
13	85	37

The more significant dust clouds are illustrated in figures 1 through 4 and are listed here by number. The horizontal dimension of each cloud was obtained by measuring the time the cloud was in the scattering volume, averaging the wind at this time with an anemometer, and hence deriving the size. The mass maxima were taken from the figures. The approximation made to obtain these mass maxima consists of the assumption that a 2-week average taken in the fall (21 micrograms per cubic meter) for mass loading (see table 2) is the same as a 2-minute average for mass loading.

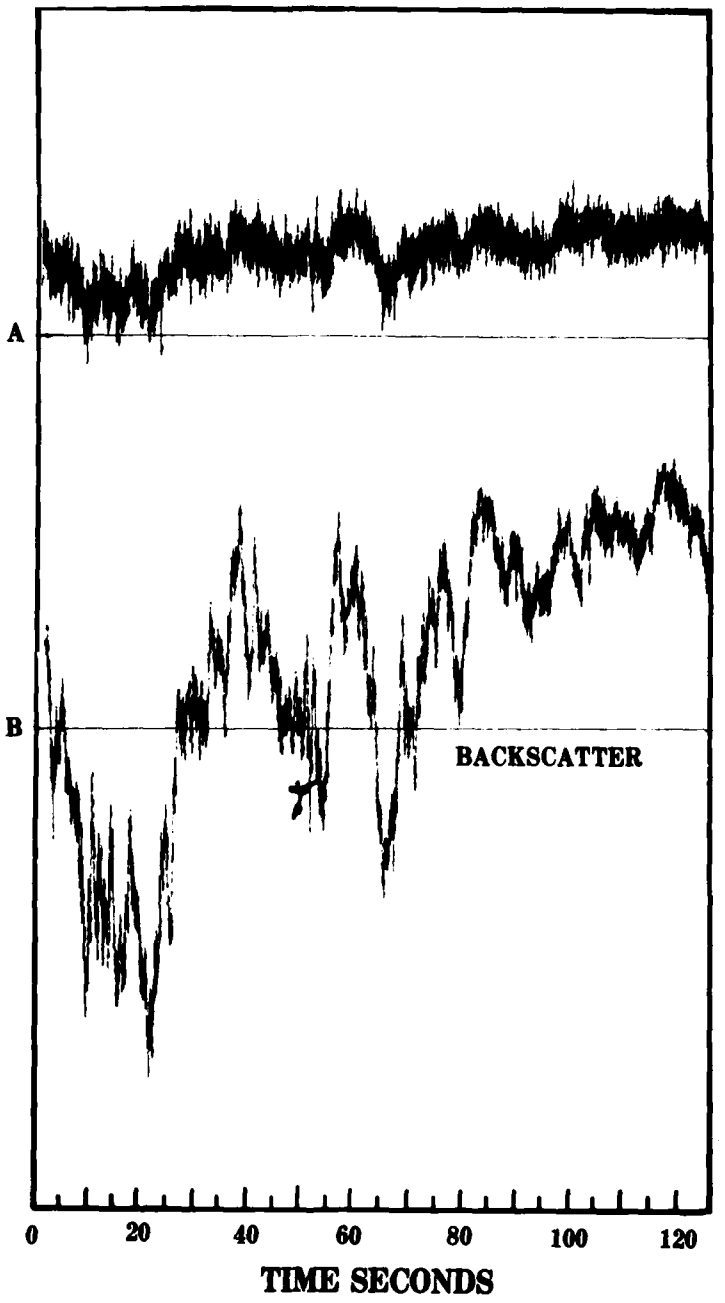

Figure 12. Backscatter data from the two lidar scattering volumes.

Two hundred points of the original data were summed and divided by 200. This was taken as one point on the graph, therefore eliminating all frequencies greater than 15 hertz. Note that, in general, the shapes of these two curves are similar. The approximate variation in amplitude of 3 is caused by: (1) a scaling factor difference of approximately 25 percent when the computer produced these two curves, (2) a slight problem of misalignment between the receiver telescope and the laser beam, and (3) a small difference in the energies between the two projected laser beams.

The results obtained here show that dust in the natural atmosphere was not perfectly mixed with the gaseous medium. Dust occurred in clouds or irregularities. In this set of data, the relative mass variation changed over a factor of approximately eight. The more predominant dust clouds are designated by numbers on figures 1 through 4 and are listed in table 3. Their estimated mass loading maximum is given with their horizontal size.

In figure 12, 2 minutes of backscattered data are presented from both of the volumes. It is evident that the general shape of both traces is similar, but possible malalignment of this transmitter beam with the atmospheric volume which the telescope was receiving is considered.

CONCLUSIONS

For the experiment reported here, the dust in the atmosphere did not form an ideal mixture with the gaseous components. For the period of time considered here, mass loading cells can be observed in the data.

A mathematical treatment is presented here relating the backscatter coefficient to the mass loading. With constant illumination (from the laser), the backscattered signal is proportional to the backscatter coefficient.

In the data presented, the clearly defined mass loading cells are pointed out as to their size and estimated mass loading maxima and are then numbered. There is an approximate factor of 8 variation in relative mass loading.

These results should be of value to studies of the atmosphere as relates to chemical reaction and energy balance where a better understanding of actual dust distribution is important.

FUTURE RESEARCH

The problem of the high frequency components in the backscattered signal should be investigated to verify if they are caused by optical turbulence in the atmosphere.

Another area of interest for future research will be to look at the backscatter from individual minerals in the dust by utilizing ordinary Raman scatter techniques.

Some of the uncertainty in this data analysis could be eliminated by taking backscatter data and Knollenberg counter data simultaneously.

REFERENCES

1. "Krakatoa," Encyclopedia Britannica, 13:498-499 (1959).

2. Fernald, F. G., and B. G. Shuster, 1977, "Wintertime 1973 Airborne Lidar Measurements of Stratospheric Aerosols," J Geophys, 82(3).

3. Collis, Ronald T. H., 1968, "Lidar Observations of Atmospheric Motion in Forest Valleys," Bull Am Meteorol Soc, 49:918.

4. Derr, V. E., and C. G. Little, 1970, "A Comparison of Remote Sensing of the Clear Atmosphere by Optical, Radio and Acoustic Radar Techniques," Appl Opt, 9(9):1976-1985.

5. Leuthner, T. G., and E. W. Eloranta, 1977, "Remote Measurements of Longitudinal and Crosspath Wind Velocities with a Monostatic Lidar," paper presented at the Eighth International Laser Radar Conference at Drexel University, Philadelphia, PA, June 1977.

6. Clebsch, A., J Fur Math, 61:195 (1863).

7. Rayleigh, Lord, 1912, The Scientific Papers of Lord Rayleigh, 1 and 4, Cambridge University Press, NY.

8. Mie, G., 1908, "Beitrag zur optik trüber medien, speziell kolloidaler metallosungen," Ann Phys, 25:377-445.

9. Debye, P., 1909, "Das verhalten von lichtwellen in der nähe eines brennpunktes oder einer brennlinie," Ann Phys, 30:755-776.

10. Kerker, M., 1969, The Scattering of Light and Other Electro-Magnetic Radiation, Academic Press, NY.

11. Hoidale, G. B., S. M. Smith, A. J. Blanco, and T. L. Barber, 1967, "A Study of Atmospheric Dust," ECOM Report 5067, Atmospheric Sciences Laboratory, White Sands Missile Range, NM.

12. Larsen, Esper S., and Harry Berman, 1934, "The Microscopic Determination of the Nonopaque Minerals," Bulletin 848, US Department of the Interior, Geological Survey.

13. Toon, Owen B., James B. Pollack, and Carl Sagan, 1977, "Physical Properties of the Particles Composing the Martian Dust Storm of 1971-1972," Icarus, 30:663-698.

14. Grams, G. W., I. H. Blifford, Jr., D. A. Gillette, and P. B. Russell, 1974, "Complex Index of Refraction of Airborne Soil Particles," J Appl Meteorol, 13:459-471.

15. Jennings, S. G., R. G. Pinnick, and J. B. Gillespie, 1979, "Relation Between Absorption Coefficients and Imaginary Index of Atmospheric Aerosol Constituents," Appl Opt, 18(9):1368-1371.

16. Lindberg, James D., and James B. Gillespie, 1977, "Relationship Between Particle Size and Imaginary Refractive Index in Atmospheric Dust," Appl Opt, 16:2628-2630.

17. Chýlek, Peter, G. W. Grams, and R. G. Pinnick, 1976, "Light Scattering by Irregular Randomly Oriented Particles," Science, 193:480-482.

18. Pinnick, R. G., D. E. Carroll, and D. J. Hofmann, 1976, "Polarized Light Scattered from Monodisperse Randomly Oriented Non-Spherical Aerosol Particles: Measurements," Appl Opt, 15(2):384-393.

19. Koschmieder, H., 1924, "Theorie der horizontalen Sichweite," Beitr Phys freien Atm, 12:33-53, 171-181.

20. Barber, T. L., and J. B. Mason, 1974, "A Transit-Time Lidar Wind Measurement: A Feasibility Study," ECOM Report 5550, Atmospheric Sciences Laboratory, White Sands Missile Range, NM.

21. Pinnick, R. G., and H. J. Auvermann, 1979, "Response Characteristics of Knollenberg Light-Scattering Aerosol Counters," J Aerosol Sci, 10:55-74.

22. Charlson, Robert J., N. C. Ahlquist, H. Selvidge, and P. B. Macready, Jr., 1969, "Monitoring of Atmospheric Aerosol Parameters with the Integrating Nephelometer," J Air Poll Control Assoc, 19:937-942.

23. Wickramasinghe, N. C., 1973, Light Scattering Functions for Small Particles with Applications in Astronomy, John Wiley and Sons, NY.

24. McClatchey, R. A., R. W. Fenn, J. E. A. Selby, F. E. Volz, and J. S. Garing, 1971, "Optical Properties of the Atmosphere (Revised)," AD 726116, AFCRL-71-0279, Environmental Research Papers, Air Force Cambridge Research Laboratories, L. C. Hanscom Field, Bedford, MA.

DEFINITION OF SYMBOLS

X	Size parameter in light-scattering theory. $X = \frac{2\pi r}{\lambda}$.
λ	The wavelength of light under consideration. In this experiment, the Cu vapor laser was producing two wavelengths, but only one wavelength, 5106 angstroms, was used.
r	The geometric radius of the particle that is causing the light scattering.
m	The index of refraction of the particle doing the scattering. $m = n - ik$.
n	The real portion of the index of refraction.
k	The imaginary part of the index of refraction. $A = \frac{4\pi k}{\lambda}$, where A is the Lambert Beer law absorption coefficient, for particles having a diameter less than the wavelength.
G	The backscatter gain for a specific particle. G is a function of m and X.
B_{180}	The effective backscattering cross section of all the particles that are being irradiated, in the scattering volume of interest. Ideally, this is the scatter parallel to the laser beam, back along it.
P	The density of the dust; this is, the density of the solid material. It is a weighted average for the minerals of which the dust is composed.
M	The total mass of dust in a specific volume of air, usually in $\mu g\ m^{-3}$.
r_2	The largest dust particle expected for the particular condition of interest. In the case used here, there is no specific limit to the maximum size.
r_1	Smallest particle radius encountered. Because of agglomeration of extremely fine particles, the minimum n is about 0.01 micron.
E	The energy output at the front of the laser in the wavelength range 5106 angstroms.
S	The total scattered signal available at the front of the receiver telescope that will enter the telescope.

V The horizontal visibility as measured by the human eye. Different objects are observed horizontally. The most distant one that can be seen is noted as to its distance from the observer.

V_1 The voltage passed from the photomultiplier to the sample and hold network. The tape recorder receives the voltage from the sample and hold network. This is an average voltage signal during the gate period from the photomultiplier.

Z The efficiency of the receiver telescope. The primary and secondary mirrors have a reflectivity of about 0.9. The optical filter has a transmission of 0.6 at 5106 angstroms. The phototube has a quantum efficiency of 30 percent at 5106 angstroms.

$f(r)$ The differential size distribution of the dust of interest. This type of size distribution will give the fraction of dust having a size r. When integrated from r_2 and r_1, the result is 1.

L The range from the lidar to the scattering volumes. This is produced by the laser putting out a pulse and the gate circuit delaying the gate to open until the pulse has traveled L, the range.

σ The atmospheric extinction, this is absorption and scatter, from the total material in the atmosphere.

A The Lambert-Beer's law coefficient absorption of light at the wavelength.

T The transmission, which is the fraction of unaffected light traveling through a specific length of the atmosphere. The light can be removed either by scattering or absorption. Ideally, this value will be 1 in a vacuum path.

T_s The sample time in seconds that the dust counter recorded the number of particles, C. In table 1, the period was 120 seconds.

r_c The average size radius of the dust particles counted in that channel of the dust counter. In the example presented, table 1, this number is listed in column 4.

C The number of particles seen and counted by the dust particle counter over a range Δr, centered at a size radius of r_c over the time period T_s. These numbers appear in table 1, column 2.

Δr The range of sizes of particles that the dust counter will see and count in one channel. Numbers are listed in table 1, column 5.

F The flow rate of air and dust through the light scattering chamber. A small fan draws the air through this sampling cavity.

N_o The total number of dust particles of all sizes in the scattering volume.

DISTRIBUTION LIST

Dr. Frank D. Eaton
Geophysical Institute
University of Alaska
Fairbanks, AK 99701

Commander
US Army Aviation Center
ATTN: ATZQ-D-MA
Fort Rucker, AL 36362

Chief, Atmospheric Sciences Div
Code ES-81
NASA
Marshall Space Flight Center,
AL 35812

Commander
US Army Missile R&D Command
ATTN: DRDMI-CGA (B. W. Fowler)
Redstone Arsenal, AL 35809

Redstone Scientific Information Center
ATTN: DRDMI-TBD
US Army Missile R&D Command
Redstone Arsenal, AL 35809

Commander
US Army Missile R&D Command
ATTN: DRDMI-TEM (R. Haraway)
Redstone Arsenal, AL 35809

Commander
US Army Missile R&D Command
ATTN: DRDMI-TRA (Dr. Essenwanger)
Redstone Arsenal, AL 35809

Commander
HQ, Fort Huachuca
ATTN: Tech Ref Div
Fort Huachuca, AZ 85613

Commander
US Army Intelligence Center & School
ATTN: ATSI-CD-MD
Fort Huachuca, AZ 85613

Commander
US Army Yuma Proving Ground
ATTN: Technical Library
Bldg 2100
Yuma, AZ 85364

Naval Weapons Center (Code 3173)
ATTN: Dr. A. Shlanta
China Lake, CA 93555

Sylvania Elec Sys Western Div
ATTN: Technical Reports Library
PO Box 205
Mountain View, CA 94040

Geophysics Officer
PMTC Code 3250
Pacific Missile Test Center
Point Mugu, CA 93042

Commander
Naval Ocean Systems Center (Code 4473)
ATTN: Technical Library
San Diego, CA 92152

Meteorologist in Charge
Kwajalein Missile Range
PO Box 67
APO San Francisco, CA 96555

Director
NOAA/ERL/APCL R31
RB3-Room 567
Boulder, CO 80302

Library-R-51-Tech Reports
NOAA/ERL
320 S. Broadway
Boulder, CO 80302

National Center for Atmos Research
NCAR Library
PO Box 3000
Boulder, CO 80307

R. B. Girardo
Bureau of Reclamation
E&R Center, Code 1220
Denver Federal Center, Bldg 67
Denver, CO 80225

National Weather Service
National Meteorological Center
W321, WWB, Room 201
ATTN: Mr. Quiroz
Washington, DC 20233

Mil Assistant for Atmos Sciences
Ofc of the Undersecretary of Defense
for Rsch & Engr/E&LS - Room 3D129
The Pentagon
Washington, DC 20301

Defense Communications Agency
Technical Library Center
Code 205
Washington, DC 20305

Director
Defense Nuclear Agency
ATTN: Technical Library
Washington, DC 20305

HQDA (DAEN-RDM/Dr. de Percin)
Washington, DC 20314

Director
Naval Research Laboratory
Code 5530
Washington, DC 20375

Commanding Officer
Naval Research Laboratory
Code 2627
Washington, DC 20375

Dr. J. M. MacCallum
Naval Research Laboratory
Code 1409
Washington, DC 20375

The Library of Congress
ATTN: Exchange & Gift Div
Washington, DC 20540
2

Head, Atmos Rsch Section
Div Atmospheric Science
National Science Foundation
1800 G. Street, NW
Washington, DC 20550

CPT Hugh Albers, Exec Sec
Interdept Committee on Atmos Science
National Science Foundation
Washington, DC 20550

Director, Systems R&D Service
Federal Aviation Administration
ATTN: ARD-54
2100 Second Street, SW
Washington, DC 20590

ADTC/DLODL
Eglin AFB, FL 32542

Naval Training Equipment Center
ATTN: Technical Library
Orlando, FL 32813

Det 11, 2WS/OI
ATTN: Maj Orondorff
Patrick AFB, FL 32925

USAFETAC/CB
Scott AFB, IL 62225

HQ, ESD/TOSI/S-22
Hanscom AFB, MA 01731

Air Force Geophysics Laboratory
ATTN: LCB (A. S. Carten, Jr.)
Hanscom AFB, MA 01731

Air Force Geophysics Laboratory
ATTN: LYD
Hanscom AFB, MA 01731

Meteorology Division
AFGL/LY
Hanscom AFB, MA 01731

US Army Liaison Office
MIT-Lincoln Lab, Library A-082
PO Box 73
Lexington, MA 02173

Director
US Army Ballistic Rsch Lab
ATTN: DRDAR-BLB (Dr. G. E. Keller)
Aberdeen Proving Ground, MD 21005

Commander
US Army Ballistic Rsch Lab
ATTN: DRDAR-BLP
Aberdeen Proving Ground, MD 21005

Director
US Army Armament R&D Command
Chemical Systems Laboratory
ATTN: DRDAR-CLJ-I
Aberdeen Proving Ground, MD 21010

Chief CB Detection & Alarms Div
Chemical Systems Laboratory
ATTN: DRDAR-CLC-CR (H. Tannenbaum)
Aberdeen Proving Ground, MD 21010

Commander
Harry Diamond Laboratories
ATTN: DELHD-CO
2800 Powder Mill Road
Adelphi, MD 20783

Commander
ERADCOM
ATTN: DRDEL-AP
2800 Powder Mill Road
Adelphi, MD 20783
2

Commander
ERADCOM
ATTN: DRDEL-CG/DRDEL-DC/DRDEL-CS
2800 Powder Mill Road
Adelphi, MD 20783

Commander
ERADCOM
ATTN: DRDEL-CT
2800 Powder Mill Road
Adelphi, MD 20783

Commander
ERADCOM
ATTN: DRDEL-EA
2800 Powder Mill Road
Adelphi, MD 20783

Commander
ERADCOM
ATTN: DRDEL-PA/DRDEL-ILS/DRDEL-E
2800 Powder Mill Road
Adelphi, MD 20783

Commander
ERADCOM
ATTN: DRDEL-PAO (S. Kimmel)
2800 Powder Mill Road
Adelphi, MD 20783

Chief
Intelligence Materiel Dev & Support Ofc
ATTN: DELEW-M-I
Bldg 4554
Fort George G. Meade, MD 20755

Acquisitions Section, IRDB-D823
Library & Info Service Div, NOAA
6009 Executive Blvd
Rockville, MD 20852

Naval Surface Weapons Center
White Oak Library
Silver Spring, MD 20910

The Environmental Research
Institute of MI
ATTN: IRIA Library
PO Box 8618
Ann Arbor, MI 48107

Mr. William A. Main
USDA Forest Service
1407 S. Harrison Road
East Lansing, MI 48823

Dr. A. D. Belmont
Research Division
PO Box 1249
Control Data Corp
Minneapolis, MN 55440

Director
Naval Oceanography & Meteorology
NSTL Station
Bay St Louis, MS 39529

Director
US Army Engr Waterways Experiment Sta
ATTN: Library
PO Box 631
Vicksburg, MS 39180

Environmental Protection Agency
Meteorology Laboratory
Research Triangle Park, NC 27711

US Army Research Office
ATTN: DRXRO-PP
PO Box 12211
Research Triangle Park, NC 27709

Commanding Officer
US Army Armament R&D Command
ATTN: DRDAR-TSS Bldg 59
Dover, NJ 07801

Commander
HQ, US Army Avionics R&D Activity
ATTN: DAVAA-O
Fort Monmouth, NJ 07703

Commander/Director
US Army Combat Surveillance & Target
Acquisition Laboratory
ATTN: DELCS-D
Fort Monmouth, NJ 07703

Commander
US Army Electronics R&D Command
ATTN: DELCS-S
Fort Monmouth, NJ 07703

US Army Materiel Systems
Analysis Activity
ATTN: DRXSY-MP
Aberdeen Proving Ground, MD 21005

Director
US Army Electronics Technology &
Devices Laboratory
ATTN: DELET-D
Fort Monmouth, NJ 07703

Commander
US Army Electronic Warfare Laboratory
ATTN: DELEW-D
Fort Monmouth, NJ 07703

Commander
US Army Night Vision &
Electro-Optics Laboratory
ATTN: DELNV-L (Dr. Rudolf Buser)
Fort Monmouth, NJ 07703

Commander
ERADCOM Technical Support Activity
ATTN: DELSD-L
Fort Monmouth, NJ 07703

Project Manager, FIREFINDER
ATTN: DRCPM-FF
Fort Monmouth, NJ 07703

Project Manager, REMBASS
ATTN: DRCPM-RBS
Fort Monmouth, NJ 07703

Commander
US Army Satellite Comm Agency
ATTN: DRCPM-SC-3
Fort Monmouth, NJ 07703

Commander
ERADCOM Scientific Advisor
ATTN: DRDEL-SA
Fort Monmouth, NJ 07703

6585 TG/WE
Holloman AFB, NM 88330

AFWL/WE
Kirtland, AFB, NM 87117

AFWL/Technical Library (SUL)
Kirtland AFB, NM 87117

Commander
US Army Test & Evaluation Command
ATTN: STEWS-AD-L
White Sands Missile Range, NM 88002

Rome Air Development Center
ATTN: Documents Library
TSLD (Bette Smith)
Griffiss AFB, NY 13441

Commander
US Army Tropic Test Center
ATTN: STETC-TD (Info Center)
APO New York 09827

Commandant
US Army Field Artillery School
ATTN: ATSF-CD-R (Mr. Farmer)
Fort Sill, OK 73503

Commandant
US Army Field Artillery School
ATTN: ATSF-CF-R
Fort Sill, OK 73503

Director CFD
US Army Field Artillery School
ATTN: Met Division
Fort Sill, OK 73503

Commandant
US Army Field Artillery School
ATTN: Morris Swett Library
Fort Sill, OK 73503

Commander
US Army Dugway Proving Ground
ATTN: MT-DA-L
Dugway, UT 84022

Dr. C. R. Sreedrahan
Research Associates
Utah State University, UNC 48
Logan, UT 84322

Inge Dirmhirn, Professor
Utah State University, UNC 48
Logan, UT 84322

Defense Documentation Center
ATTN: DDC-TCA
Cameron Station Bldg 5
Alexandria, VA 22314
12

Commanding Officer
US Army Foreign Sci & Tech Center
ATTN: DRXST-IS1
220 7th Street, NE
Charlottesville, VA 22901

Naval Surface Weapons Center
Code G65
Dahlgren, VA 22448

Commander
US Army Night Vision
& Electro-Optics Lab
ATTN: DELNV-D
Fort Belvoir, VA 22060

Commander and Director
US Army Engineer Topographic Lab
ETL-TD-MB
Fort Belvoir, VA 22060

Director
Applied Technology Lab
DAVDL-EU-TSD
ATTN: Technical Library
Fort Eustis, VA 23604

Department of the Air Force
OL-C, 5WW
Fort Monroe, VA 23651

Department of the Air Force
5WW/DN
Langley AFB, VA 23665

Director
Development Center MCDEC
ATTN: Firepower Division
Quantico, VA 22134

US Army Nuclear & Chemical Agency
ATTN: MONA-WE
Springfield, VA 22150

Director
US Army Signals Warfare Laboratory
ATTN: DELSW-OS (Dr. R. Burkhardt)
Vint Hill Farms Station
Warrenton, VA 22186

Commander
US Army Cold Regions Test Center
ATTN: STECR-OP-PM
APO Seattle, WA 98733

Dr. John L. Walsh
Code 5560
Navy Research Lab
Washington, DC 20375

Commander
TRASANA
ATTN: ATAA-PL
(Dolores Anguiano)
White Sands Missile Range, NM 88002

Commander
US Army Dugway Proving Ground
ATTN: STEDP-MT-DA-M (Mr. Paul Carlson)
Dugway, UT 84022

Commander
US Army Dugway Proving Ground
ATTN: STEDP-MT-DA-T
(Mr. William Peterson)
Dugway, UT 84022

Commander
USATRADOC
ATTN: ATCD-SIE
Fort Monroe, VA 23651

Commander
USATRADOC
ATTN: ATCD-CF
Fort Monroe, VA 23651

Commander
USATRADOC
ATTN: Tech Library
Fort Monroe, VA 23651

ATMOSPHERIC SCIENCES RESEARCH PAPERS

1. Lindberg, J.D., "An Improvement to a Method for Measuring the Absorption Coefficient of Atmospheric Dust and other Strongly Absorbing Powders, " ECOM-5565, July 1975.
2. Avara, Elton, P., "Mesoscale Wind Shears Derived from Thermal Winds," ECOM-5566, July 1975.
3. Gomez, Richard B., and Joseph H. Pierluissi, "Incomplete Gamma Function Approximation for King's Strong-Line Transmittance Model," ECOM-5567, July 1975.
4. Blanco, A.J., and B.F. Engebos, "Ballistic Wind Weighting Functions for Tank Projectiles," ECOM-5568, August 1975.
5. Taylor, Fredrick J., Jack Smith, and Thomas H. Pries, "Crosswind Measurements through Pattern Recognition Techniques," ECOM-5569, July 1975.
6. Walters, D.L., "Crosswind Weighting Functions for Direct-Fire Projectiles," ECOM-5570, August 1975.
7. Duncan, Louis D., "An Improved Algorithm for the Iterated Minimal Information Solution for Remote Sounding of Temperature," ECOM-5571, August 1975.
8. Robbiani, Raymond L., "Tactical Field Demonstration of Mobile Weather Radar Set AN/TPS-41 at Fort Rucker, Alabama," ECOM-5572, August 1975.
9. Miers, B., G. Blackman, D. Langer, and N. Lorimier, "Analysis of SMS/GOES Film Data," ECOM-5573, September 1975.
10. Manquero, Carlos, Louis Duncan, and Rufus Bruce, "An Indication from Satellite Measurements of Atmospheric CO2 Variability," ECOM-5574, September 1975.
11. Petracca, Carmine, and James D. Lindberg, "Installation and Operation of an Atmospheric Particulate Collector," ECOM-5575, September 1975.
12. Avara, Elton P., and George Alexander, "Empirical Investigation of Three Iterative Methods for Inverting the Radiative Transfer Equation," ECOM-5576, October 1975.
13. Alexander, George D., "A Digital Data Acquisition Interface for the SMS Direct Readout Ground Station — Concept and Preliminary Design," ECOM-5577, October 1975.
14. Cantor, Israel, "Enhancement of Point Source Thermal Radiation Under Clouds in a Nonattenuating Medium," ECOM-5578, October 1975.
15. Norton, Colburn, and Glenn Hoidale, "The Diurnal Variation of Mixing Height by Month over White Sands Missile Range, N.M," ECOM-5579, November 1975.
16. Avara, Elton P., "On the Spectrum Analysis of Binary Data," ECOM-5580, November 1975.
17. Taylor, Fredrick J., Thomas H. Pries, and Chao-Huan Huang, "Optimal Wind Velocity Estimation," ECOM-5581, December 1975.
18. Avara, Elton P., "Some Effects of Autocorrelated and Cross-Correlated Noise on the Analysis of Variance, " ECOM-5582, December 1975.
19. Gillespie, Patti S., R.L. Armstrong, and Kenneth O. White, "The Spectral Characteristics and Atmospheric CO2 Absorption of the Ho^{+3}:YLF Laser at 2.05μm," ECOM-5583, December 1975.
20. Novlan, David J. "An Empirical Method of Forecasting Thunderstorms for the White Sands Missile Range," ECOM-5584, February 1976.
21. Avara, Elton P., "Randomization Effects in Hypothesis Testing with Autocorrelated Noise," ECOM-5585, February 1976.
22. Watkins, Wendell R., "Improvements in Long Path Absorption Cell Measurement," ECOM-5586, March 1976.
23. Thomas, Joe, George D. Alexander, and Marvin Dubbin, "SATTEL — An Army Dedicated Meteorological Telemetry System," ECOM-5587, March 1976.
24. Kennedy, Bruce W., and Delbert Bynum, "Army User Test Program for the RDT&E-XM-75 Meteorological Rocket," ECOM-5588, April 1976.

25. Barnett, Kenneth M., "A Description of the Artillery Meteorological Comparisons at White Sands Missle Range, October 1974 - December 1974 ('PASS' - Prototype Artillery [Meteorological] Subsystem)," ECOM-5589, April 1976.
26. Miller, Walter B., "Preliminary Analysis of Fall-of-Shot From Project 'PASS'," ECOM-5590, April 1976.
27. Avara, Elton P., "Error Analysis of Minimum Information and Smith's Direct Methods for Inverting the Radiative Transfer Equation," ECOM-5591, April 1976.
28. Yee, Young P., James D. Horn, and George Alexander, "Synoptic Thermal Wind Calculations from Radiosonde Observations Over the Southwestern United States," ECOM-5592, May 1976.
29. Duncan, Louis D., and Mary Ann Seagraves, "Applications of Empirical Corrections to NOAA-4 VTPR Observations," ECOM-5593, May 1976.
30. Miers, Bruce T., and Steve Weaver, "Applications of Meterological Satellite Data to Weather Sensitive Army Operations,"ECOM-5594, May 1976.
31. Sharenow, Moses, "Redesign and Improvement of Balloon ML-566," ECOM-5595, June, 1976.
32. Hansen, Frank V., "The Depth of the Surface Boundary Layer," ECOM-5596, June 1976.
33. Pinnick, R.G., and E.B. Stenmark, "Response Calculations for a Commercial Light-Scattering Aerosol Counter," ECOM-5597, July 1976.
34. Mason, J., and G.B. Hoidale, "Visibility as an Estimator of Infrared Transmittance," ECOM-5598, July 1976.
35. Bruce, Rufus E., Louis D. Duncan, and Joseph H. Pierluissi, "Experimental Study of the Relationship Between Radiosonde Temperatures and Radiometric-Area Temperatures," ECOM-5599, August 1976.
36. Duncan, Louis D., "Stratospheric Wind Shear Computed from Satellite Thermal Sounder Measurements," ECOM-5800, September 1976.
37. Taylor, F., P. Mohan, P. Joseph and T. Pries, "An All Digital Automated Wind Measurement System," ECOM-5801, September 1976.
38. Bruce, Charles, "Development of Spectrophones for CW and Pulsed Radiation Sources," ECOM-5802, September 1976.
39. Duncan, Louis D., and Mary Ann Seagraves,"Another Method for Estimating Clear Column Radiances," ECOM-5803, October 1976.
40. Blanco, Abel J., and Larry E. Taylor, "Artillery Meteorological Analysis of Project Pass," ECOM-5804, October 1976.
41. Miller, Walter, and Bernard Engebos," A Mathematical Structure for Refinement of Sound Ranging Estimates," ECOM-5805, November, 1976.
42. Gillespie, James B., and James D. Lindberg, "A Method to Obtain Diffuse Reflectance Measurements from 1.0 to 3.0 μm Using a Cary 17I Spectrophotometer," ECOM-5806, November 1976.
43. Rubio, Roberto, and Robert O. Olsen,"A Study of the Effects of Temperature Variations on Radio Wave Absorption,"ECOM-5807, November 1976.
44. Ballard, Harold N., "Temperature Measurements in the Stratosphere from Balloon-Borne Instrument Platforms, 1968-1975," ECOM-5808, December 1976.
45. Monahan, H.H., "An Approach to the Short-Range Prediction of Early Morning Radiation Fog," ECOM-5809, January 1977.
46. Engebos, Bernard Francis, "Introduction to Multiple State Multiple Action Decision Theory and Its Relation to Mixing Structures," ECOM-5810, January 1977.
47. Low, Richard D.H.,"Effects of Cloud Particles on Remote Sensing from Space in the 10-Micrometer Infrared Region," ECOM-5811, January 1977.
48. Bonner, Robert S., and R. Newton, "Application of the AN/GVS-5 Laser Rangefinder to Cloud Base Height Measurements," ECOM-5812, February 1977.
49. Rubio, Roberto, "Lidar Detection of Subvisible Reentry Vehicle Erosive Atmospheric Material," ECOM-5813, March 1977.
50. Low, Richard D.H., and J.D. Horn, "Mesoscale Determination of Cloud-Top Height: Problems and Solutions," ECOM-5814, March 1977.

51. Duncan, Louis D., and Mary Ann Seagraves,"Evaluation of the NOAA-4 VTPR Thermal Winds for Nuclear Fallout Predictions," ECOM-5815, March 1977.
52. Randhawa, Jagir S., M. Izquierdo, Carlos McDonald and Zvi Salpeter, "Stratospheric Ozone Density as Measured by a Chemiluminescent Sensor During the Stratcom VI-A Flight," ECOM-5816, April 1977.
53. Rubio, Roberto, and Mike Izquierdo, "Measurements of Net Atmospheric Irradiance in the 0.7- to 2.8-Micrometer Infrared Region," ECOM-5817, May 1977.
54. Ballard, Harold N., Jose M. Serna, and Frank P. Hudson Consultant for Chemical Kinetics, "Calculation of Selected Atmospheric Composition Parameters for the Mid-Latitude, September Stratosphere," ECOM-5818, May 1977.
55. Mitchell, J.D., R.S. Sagar, and R.O. Olsen, "Positive Ions in the Middle Atmosphere During Sunrise Conditions," ECOM-5819, May 1977.
56. White, Kenneth O., Wendell R. Watkins, Stuart A. Schleusener, and Ronald L. Johnson, "Solid-State Laser Wavelength Identification Using a Reference Absorber," ECOM-5820, June 1977.
57. Watkins, Wendell R., and Richard G. Dixon, "Automation of Long-Path Absorption Cell Measurements," ECOM-5821, June 1977.
58. Taylor, S.E., J.M. Davis, and J.B. Mason, "Analysis of Observed Soil Skin Moisture Effects on Reflectance," ECOM-5822, June 1977.
59. Duncan, Louis D. and Mary Ann Seagraves, "Fallout Predictions Computed from Satellite Derived Winds," ECOM-5823, June 1977.
60. Snider, D.E., D.G. Murcray, F.H. Murcray, and W.J. Williams, "Investigation of High-Altitude Enhanced Infrared Backround Emissions" (U), SECRET, ECOM-5824, June 1977.
61. Dubbin, Marvin H. and Dennis Hall, "Synchronous Meteorlogical Satellite Direct Readout Ground System Digital Video Electronics," ECOM-5825, June 1977.
62. Miller, W., and B. Engebos, "A Preliminary Analysis of Two Sound Ranging Algorithms," ECOM-5826, July 1977.
63. Kennedy, Bruce W., and James K. Luers, "Ballistic Sphere Techniques for Measuring Atomspheric Parameters," ECOM-5827, July 1977.
64. Duncan, Louis D., "Zenith Angle Variation of Satellite Thermal Sounder Measurements," ECOM-5828, August 1977.
65. Hansen, Frank V., "The Critical Richardson Number," ECOM-5829, September 1977.
66. Ballard, Harold N., and Frank P. Hudson (Compilers), "Stratospheric Composition Balloon-Borne Experiment," ECOM-5830, October 1977.
67. Barr, William C., and Arnold C. Peterson, "Wind Measuring Accuracy Test of Meteorological Systems," ECOM-5831, November 1977.
68. Ethridge, G.A. and F.V. Hansen, "Atmospheric Diffusion: Similarity Theory and Empirical Derivations for Use in Boundary Layer Diffusion Problems," ECOM-5832, November 1977.
69. Low, Richard D.H., "The Internal Cloud Radiation Field and a Technique for Determining Cloud Blackness," ECOM-5833, December 1977.
70. Watkins, Wendell R., Kenneth O. White, Charles W. Bruce, Donald L. Walters, and James D. Lindberg, "Measurements Required for Prediction of High Energy Laser Transmission," ECOM-5834, December 1977.
71. Rubio, Robert, "Investigation of Abrupt Decreases in Atmospherically Backscattered Laser Energy," ECOM-5835, December 1977.
72. Monahan, H.H. and R.M. Cionco, "An Interpretative Review of Existing Capabilities for Measuring and Forecasting Selected Weather Variables (Emphasizing Remote Means)," ASL-TR-0001, January 1978.
73. Heaps, Melvin G., "The 1979 Solar Eclipse and Validation of D-Region Models," ASL-TR-0002. March 1978.

74. Jennings, S.G., and J.B. Gillespie, "M I.E. Theory Sensitivity Studies - The Effects of Aerosol Complex Refractive Index and Size Distribution Variations on Extinction and Absorption Coefficients Part II: Analysis of the Computational Results," ASL-TR-0003, March 1978.
75. White, Kenneth O. et al, "Water Vapor Continuum Absorption in the 3.5μm to 4.0μm Region," ASL-TR-0004, March 1978.
76. Olsen, Robert O., and Bruce W. Kennedy, "ABRES Pretest Atmospheric Measurements," ASL-TR-0005, April 1978.
77. Ballard, Harold N., Jose M. Serna, and Frank P. Hudson, "Calculation of Atmospheric Composition in the High Latitude September Stratosphere," ASL-TR-0006, May 1978.
78. Watkins, Wendell R. et al, "Water Vapor Absorption Coefficients at HF Laser Wavelengths," ASL-TR-0007, May 1978.
79. Hansen, Frank V., "The Growth and Prediction of Nocturnal Inversions," ASL-TR-0008, May 1978.
80. Samuel, Christine, Charles Bruce, and Ralph Brewer, "Spectrophone Analysis of Gas Samples Obtained at Field Site," ASL-TR-0009, June 1978.
81. Pinnick, R.G. et al., "Vertical Structure in Atmospheric Fog and Haze and its Effects on IR Extinction," ASL-TR-0010, July 1978.
82. Low, Richard D.H., Louis D. Duncan, and Richard B. Gomez, "The Microphysical Basis of Fog Optical Characterization," ASL-TR-0011, August 1978.
83. Heaps, Melvin G., "The Effect of a Solar Proton Event on the Minor Neutral Constituents of the Summer Polar Mesosphere," ASL-TR-0012, August 1978.
84. Mason, James B., "Light Attenuation in Falling Snow," ASL-TR-0013, August 1978.
85. Blanco, Abel J., "Long-Range Artillery Sound Ranging: "PASS" Meteorological Application," ASL-TR-0014, September 1978.
86. Heaps, M.G., and F.E. Niles, "Modeling the Ion Chemistry of the D-Region: A case Study Based Upon the 1966 Total Solar Eclipse," ASL-TR-0015, September 1978.
87. Jennings, S.G., and R.G. Pinnick, "Effects of Particulate Complex Refractive Index and Particle Size Distribution Variations on Atmospheric Extinction and Absorption for Visible Through Middle-Infrared Wavelengths," ASL-TR-0016, September 1978.
88. Watkins, Wendell R., Kenneth O. White, Lanny R. Bower, and Brian Z. Sojka, " Pressure Dependence of the Water Vapor Continuum Absorption in the 3.5- to 4.0-Micrometer Region," ASL-TR-0017, September 1978.
89. Miller, W.B., and B.F. Engebos, "Behavior of Four Sound Ranging Techniques in an Idealized Physical Enviroment," ASL-TR-0018, September 1978.
90. Gomez, Richard G., "Effectiveness Studies of the CBU-88/B Bomb, Cluster, Smoke Weapon" (U), CONFIDENTIAL ASL-TR-0019, September 1978.
91. Miller, August, Richard C. Shirkey, and Mary Ann Seagraves, "Calculation of Thermal Emission from Aerosols Using the Doubling Technique," ASL-TR-0020, November, 1978.
92. Lindberg, James D. et al., "Measured Effects of Battlefield Dust and Smoke on Visible, Infrared, and Millimeter Wavelengths Propagation: A Preliminary Report on Dusty Infrared Test-I (DIRT-I)," ASL-TR-0021, January 1979.
93. Kennedy, Bruce W., Arthur Kinghorn, and B.R. Hixon, "Engineering Flight Tests of Range Meteorological Sounding System Radiosonde," ASL-TR-0022, February 1979.
94. Rubio, Roberto, and Don Hoock, "Microwave Effective Earth Radius Factor Variability at Wiesbaden and Balboa," ASL-TR-0023, February 1979.
95. Low, Richard D.H., "A Theoretical Investigation of Cloud/Fog Optical Properties and Their Spectral Correlations," ASL-TR-0024, February 1979.

96. Pinnick, R.G., and H.J. Auvermann, "Response Characteristics of Knollenberg Light-Scattering Aerosol Counters," ASL-TR-0025, February 1979.
97. Heaps, Melvin G., Robert O. Olsen, and Warren W. Berning, "Solar Eclipse 1979, Atmospheric Sciences Laboratory Program Overview," ASL-TR-0026 February 1979.
98. Blanco, Abel J., "Long-Range Artillery Sound Ranging: 'PASS' GR-8 Sound Ranging Data," ASL-TR-0027, March 1979.
99. Kennedy, Bruce W., and Jose M. Serna, "Meteorological Rocket Network System Reliability," ASL-TR-0028, March 1979.
100. Swingle, Donald M., "Effects of Arrival Time Errors in Weighted Range Equation Solutions for Linear Base Sound Ranging," ASL-TR-0029, April 1979.
101. Umstead, Robert K., Ricardo Pena, and Frank V. Hansen, "KWIK: An Algorithm for Calculating Munition Expenditures for Smoke Screening/Obscuration in Tactical Situations," ASL-TR-0030, April 1979.
102. D'Arcy, Edward M., "Accuracy Validation of the Modified Nike Hercules Radar," ASL-TR-0031, May 1979.
103. Rodriguez, Ruben, "Evaluation of the Passive Remote Crosswind Sensor," ASL-TR-0032, May 1979.
104. Barber, T.L., and R. Rodgriquez, "Transit Time Lidar Measurement of Near-Surface Winds in the Atmosphere," ASL-TR-0033, May 1979.
105. Low, Richard D.H., Louis D. Duncan, and Y.Y. Roger R. Hsiao, "Microphysical and Optical Properties of California Coastal Fogs at Fort Ord," ASL-TR-0034, June 1979.
106. Rodriguez, Ruben, and William J. Vechione, "Evaluation of the Saturation Resistant Crosswind Sensor," ASL-TR-0035, July 1979.
107. Ohmstede, William D., "The Dynamics of Material Layers," ASL-TR-0036, July 1979.
108. Pinnick, R.G., S.G. Jennings, Petr Chylek, and H.J. Auvermann "Relationships between IR Extinction, Absorption, and Liquid Water Content of Fogs," ASL-TR-0037, August 1979.
109. Rodriguez, Ruben, and William J. Vechione, "Performance Evaluation of the Optical Crosswind Profiler," ASL-TR-0038, August 1979.
110. Miers, Bruce T., "Precipitation Estimation Using Satellite Data" ASL-TR-0039, September 1979.
111. Dickson, David H., and Charles M. Sonnenschein, "Helicopter Remote Wind Sensor System Description," ASL-TR-0040, September 1979.
112. Heaps, Melvin, G., and Joseph M. Heimerl, "Validation of the Dairchem Code, I: Quiet Midlatitude Conditions," ASL-TR-0041, September 1979.
113. Bonner, Robert S., and William J. Lentz, "The Visioceilometer: A Portable Cloud Height and Visibility Indicator," ASL-TR-0042, October 1979.
114. Cohn, Stephen L., "The Role of Atmospheric Sulfates in Battlefield Obscurations," ASL-TR-0043, October 1979.
115. Fawbush, E.J. et al, "Characterization of Atmospheric Conditions at the High Energy Laser System Test Facility (HELSTF), White Sands Missile Range, New Mexico, Part I, 24 March to 8 April 1977," ASL-TR-0044, November 1979
116. Barber, Ted L., "Short-Time Mass Variation in Natural Atmospheric Dust," ASL-TR-0045, November 1979

☆ U.S. GOVERNMENT PRINTING OFFICE: 1979 — 677-119/48